

NUCLEAR SCIENCE ABSTRACTS

PUBLISHED DOCUMENTS INDEX

Document	Journal
MDDC - 859	<u>Phys Rev</u> <u>75</u> 619-623 (1949) Feb 15
MDDC - 1089	<u>Phys Rev</u> <u>75</u> 619-623 (1949) Feb 15
MDDC - 1190	<u>Phys Rev</u> <u>75</u> 619-623 (1949) Feb 15
MDDC - 1354	<u>Phys Rev</u> <u>75</u> 537-541 (1949) Feb 15
AECD - 2254	<u>J Biol Chem</u> <u>177</u> 975-984 (1949) Feb
AECD - 2340	<u>Phys Rev</u> <u>75</u> 537-541 (1949) Feb 15
AECD - 2343	<u>Phys Rev</u> <u>75</u> 578-580 (1949) Feb 15
AECD - 2363	<u>Phys Rev</u> <u>75</u> 565-569 (1949) Feb 15
AECD - 2369	<u>Phys Rev</u> <u>75</u> 555-564 (1949) Feb 15
NRC - 1858	<u>Can J Research</u> <u>27B</u> 1-5 (1949) Jan

STUDIES IN MOLECULAR STRUCTURE AND VALENCE STATE ENERGY

Thesis by
William Francis Sheehan, Jr.

In Partial Fulfillment of the Requirements
for the Degree of
Doctor of Philosophy

California Institute of Technology
Pasadena, California

1952

ACKNOWLEDGEMENT

To Professor Linus Pauling I owe thanks not only for his sharing of his concept of the valence state and his suggesting a study of the structure of molybdenum hexacarbonyl but also do I especially owe him thanks for his very generous and timely encouragement to persevere in my graduate study.

To Professor Verner Schomaker, under whose diligent direction most of this research has been conducted, and to whom I looked confidently for help in many difficulties, belongs all of this thesis. To him I give my most gracious thanks.

And to all my teachers at Caltech, especially Doctors David P. Shoemaker and Kenneth W. Hedberg, and to all my teachers at Loyola of Chicago, I must give thanks for preparing me for this research. The Shell Fellowship Committee and The United States Rubber Company have given me very generous fellowships; to them I am very grateful.

ABSTRACT

The structures of six gaseous molecules, trifluoromethylacetylene, perfluorobutyne-2, tetramethylsilane, tungsten hexacarbonyl, molybdenum hexacarbonyl, and osmium tetroxide, have been determined from a study of their electron diffraction patterns by the visual correlation method employed in these Laboratories. An interpretation of the interesting features of the unusual structures of the hexacarbonyls and the tetroxide is given. This thesis concludes with a discussion of the energies of the valence states of atoms as they exist in diatomic molecules.

TABLE OF CONTENTS

<u>PART</u>	<u>TITLE</u>	<u>PAGE</u>
I	THE STRUCTURES OF SEVERAL GASEOUS MOLECULES	1
	A. Introduction	1
	B. Trifluoromethylacetylene	2
	C. Perfluorobutyne-2	13
	D. Tetramethylsilane	24
	E. Tungsten Hexacarbonyl	26
	F. Molybdenum Hexacarbonyl	39
	G. Osmium Tetroxide	45
	References of Section I	54
II	MOLECULES WITH MULTIPLE VIBRATIONAL POTENTIAL MINIMA: MoF ₆ , WF ₆ , UF ₆ , Mo(CO) ₆ , W(CO) ₆ , OsO ₄	56
	A. The Equivalence of Non-equivalent Ligates	56
	B. The Nature of the Non-equivalent Bonds	71
	References of Section II	74
III	THE DISSOCIATION ENERGIES OF DIATOMIC MOLECULES AND THE ENERGIES OF THE VALENCE STATES OF ATOMS	75
	A. The Dissociation Energy of Carbon Monoxide and the Heat of Sublimation of Graphite	75
	B. The Energies of the Valence States of Several Atoms and the Valence State Dissociation Limits of Several Diatomic Molecules	80
	References of Section III	86
	PROPOSITIONS	87
	References of Propositions	88

I. THE STRUCTURES OF SEVERAL GASEOUS MOLECULES

A. Introduction

Photographs of the electron diffraction patterns of the several molecules were taken with the apparatus described by Brockway⁽¹⁾ and interpreted visually by the methods currently used in these Laboratories⁽²⁾. The electron wavelength was calibrated by means of zinc oxide⁽³⁾ and corrections for film expansion were made in all cases.

Radial distribution curves were calculated by means of the equation^(4,5)

$$r D(r) = \sum_{q=1,2,\dots}^{q_{\max}} I(q) e^{-aq^2} \sin(\pi qr/10)$$

with the use of punched cards^(5,6). The visual intensity curve, $I(q)$, represents the visual appearance of the photographs, and the constant a was so chosen that the quantity e^{-aq^2} was equal to 0.10 at that value of q at which the last visible feature was measured. Heavy lines beneath the radial distribution curves indicate by their positions and heights the distances and scattering weights of the best models.

Theoretical intensity curves for use in the correlation method were calculated^(5,6) usually in the $Z_i Z_j$ approximation to the equation⁽⁴⁾

$$I(q) = \frac{1}{\langle (Z-f)^2 \rangle_{AV}} \sum_{i,j} \frac{(Z-f)_i (Z-f)_j}{r_{ij}} e^{-a_{ij} q^2} \sin(\pi r_{ij} q/10).$$

Critical marks added to these theoretical intensity curves indicate tersely a qualitative or quantitative difference between each of them and some standard intensity curve, the visual curve unless explicitly noted otherwise. The use of these critical marks is indicated in detail in Table I of Section C. for the case of their first appearance, Figure 2.

In all determinations except trifluoromethylacetylene, the quoted limit of error for a shape parameter (a bond angle or a ratio of interatomic distances) is that directly determined in the correlation procedure; for an interatomic distance it is the sum of the uncertainty which arises because of the uncertainty in the shape determination and of an allowance for an estimated percentage limit of error in the scale determination.

B. Trifluoromethylacetylene

Substituted acetylenes have long been known to manifest pronounced shortening of the single-bond distances adjacent to the triple bond; this has been confirmed in several cases by recent microwave studies^(7,8). Structures of fluorocarbons have been reported⁽⁹⁾ with rather widely differing CF distances and with the hint that the FCF angle is less than tetrahedral. Of interest in all these respects is trifluoromethylacetylene, for which the CF distance has been reported⁽⁸⁾ to be 1.330\AA and the CC distance, 1.493\AA on the basis of microwave measurements on two

TABLE I

Explanation of Critical Marks of Figure 2.

Curve	Position	Mark	Meaning
A	7 max	Black dot	Inner slope should be more convex upwards. Creation operator.
B	All max, all min	Arrows	Position of maxima and minima as measured from photographs, corrected by scale factor. Best curve.
C	5 max	Black dot White dot	5 max should be found farther downwards and to the left. White dot is destruction operator.
C	9 min, 10 min	Line	9 min is too deep; 10 min, too shallow. Depths should be as line indicates.
C	9 max	Arrow	9 max is significantly misplaced relative to adjacent features. The arrow is the same as the one shown on the best curve.
C	10 max, 11 max	Terminated line	Feature should be wider, with approximate width as indicated.
D	5 min- 9 min	Curved line	8 min should lie below a line from 5 min to 9 min with relative depths as indicated.
E	8 min	Line	Feature in bottom of 8 min should lie closer to 8 max than to 7 max.
E	10 max	Cross	Completely unacceptable feature; compare standard.
F	6 max, 7 max	Line	7 max is too high relative to 6 max. Line indicates desired heights.
F	13 max	Line	13 max should lie between minima of almost equal depth.
K	4 max- 7 max	Curved line	6 max is too high relative to 4 max and 7 max. Heights should lie along curve.
K	9 max- 11 max	Line	Region should slope upwards more gently.

isotopic species and the assumptions that CH is $1.056\overset{\text{O}}{\text{\AA}}$, triple-bond CC is $1.207\overset{\text{O}}{\text{\AA}}$, and the FCF angle is tetrahedral. However, work in these laboratories⁽¹⁰⁾ on the microwave spectrum has provided four moments of inertia from the several isotopic species available, and the remaining parameter has been determined from the electron diffraction pattern.

The sample of trifluoromethylacetylene (heat of vaporization and extrapolated B.P. from vapor pressure-temperature measurements, 4650 cal/mole and -44° ; lit.⁽¹¹⁾ B.P., $-46\pm 2^{\circ}$) was furnished for both microwave and diffraction studies by Professor Albert L. Henne of The Ohio State University. Sample bulb temperatures ranged from -68° to -100° ; the electron wavelength was $0.06063\overset{\text{O}}{\text{\AA}}$ and the camera distance, 10.94 cm.

Theoretical intensity curves were calculated for models consistent with the microwave data of Table II for FCF angles in the range 106.5° to 112.5° and the three sets of temperature factor coefficients of Table III. Curves for FCF angles of 107.5° with further variations of the temperature factors for C'F and C''F were also calculated. The significant variations, however, are those shown in Table III.

Models 110.5°A and 110.5°C are clearly unacceptable in the region of maxima 8 - 11 and in the relative heights of maxima 2, 3, 4, and 5. Only models with the FCF angle less than 108.5° are acceptable if maximum 8 is to be considerably

TABLE II

Microwave Data, Trifluoromethylacetylene, $\text{CF}_3\text{C}'\text{C}''\text{H}$

FCF Angle	CF ($\overset{\text{O}}{\text{A}}$)	CC' ($\overset{\text{O}}{\text{A}}$)	C'C'' ($\overset{\text{O}}{\text{A}}$)	C''H ($\overset{\text{O}}{\text{A}}$)
106.5°	1.341	1.446	1.201	1.056
107.5°	1.335	1.464	1.201	1.056
108.5°	1.330	1.482	1.201	1.056
109.5°	1.325	1.501	1.201	1.056
110.5°	1.320	1.521	1.201	1.056
111.5°	1.315	1.542	1.201	1.056
112.5°	1.310	1.563	1.201	1.056

TABLE III

Relative Temperature Factor Coefficients, Trifluoromethyl-
acetylene, $\text{CF}_3\text{C}'\text{C}''\text{H}$

Atom Pair	$a_{ij} \times 10^4$		
	A	B	C
CF	0.2	0.2	0.2
C'F	1.0	0.9	2.1
C''F	2.0	2.6	5.5
FF	0.7	0.7	1.0
FH	5.9	7.2	7.7
CC'	0.1	0.1	0.1
CC''	0.5	0.5	0.5
C'C''	0.0	0.0	0.0
CH	3.0	3.0	3.0
C'H	2.6	2.6	2.6
C''H	2.2	2.2	2.2

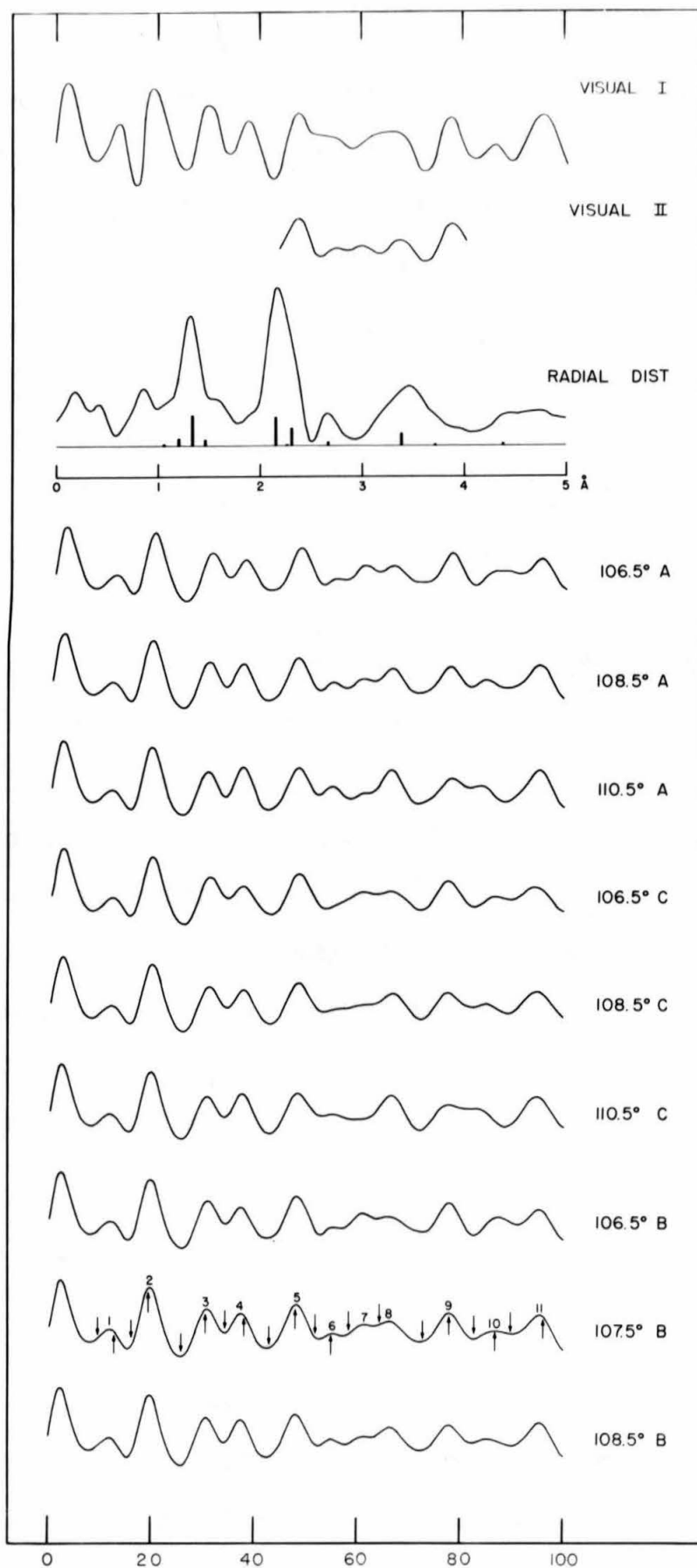


Figure 1. Trifluoromethylacetylene

weaker than maximum 9. Since maxima 6, 7, and 8 appear to increase in intensity in the order 6, 7, 8, models with the FCF angle less than 106.5° are unacceptable. Besides, a weak ring appears at about q equals 72 on model $106.5^{\circ}A$, and maximum 7 disappears in $106.5^{\circ}C$: two objections to 106.5° models which, however, could perhaps be overcome by careful adjustment of the temperature factors.

Maximum 10 and the neighboring minima change very rapidly with FCF angle and so are very important for the choice of best value and limits of error. According to visual I they would lead to a choice of about 108° , but it is not certain that the relative depths of the minima are just those shown: the photographs sometimes give the impression that minimum 11 is the shallower, possibly by as much as would correspond to an angle of 107° . The position of maximum 10 seems to afford the most sensitive indication, the measured value (which seems to be quite precise) definitely favoring the 107.5° models over all others. In general, all the 107.5° curves calculated are in good agreement with the visual curve. The lack of agreement in the relative depths of minima 2 and 3 and of minima 6 and 7 apparently cannot be resolved by changes in the model and presumably arise from errors in the visual curve. Having inspected the theoretical intensity curves before studying the photographs, Professor Schomaker was unable to make as unbiased an interpretation as was desired, but it seems

obvious to him that minimum 6 is very much deeper than shown in visual I. Dr. Kenneth Hedberg, who was unacquainted with the details of the investigation, was asked to examine the photographs over the region between what are here labeled maxima 5 to 9. His representation, visual II, confirms the conclusion that visual I is in error in regard to the depths of minima 6 and 7. It seems to be true, however, that the relative depths of minima 7 and 8 are indicated more correctly by visual I than by visual II.

Table IV shows the comparison of measured q values with those of 107.5°B . The average deviations for 106.5°B and 108.5°B are 0.0075 and 0.0074, both somewhat greater than that, 0.0057, for 107.5°B . The value of the scale factor, 1.002, is in excellent agreement with the microwave data; it has not been used to fix the scale of the molecule. This scale factor is satisfactorily stable with respect to changes in the weights, and, perhaps significantly, more so for 107.5°B than for any of the other curves. The scale factor becomes exactly unity for 108.5°B , again in general confirmation of the angle determination.

The structure of trifluoromethylacetylene, with limits of error, is given in Table V. The CF , CC' and FCF angle values are less certain than the $\text{C}'\text{C}''$ and $\text{C}''\text{H}$ values because the electron diffraction data merely restrict the three related parameters not completely fixed by the spectrum to a region of parameter space of size corresponding to the listed limits of error.

TABLE IV
Scale Factor, Trifluoromethylacetylene

Min	Max	q_{obs}	$q_{\text{calc}}/q_{\text{obs}}(107.5^{\circ}\text{B})$	Weight
1		9.5	0.844	0
	1	12.6	0.942	0
2		15.9	0.961	0
	2	19.2	1.019	1
3		25.7	1.001	2
	3	30.3	1.017	1
4		34.17	1.002	2
	4	37.9	0.987	1
5		42.8	0.989	2
	5	47.8	1.009	2
6		51.7	1.016	0
	6	54.8	1.008	0
7		58.1	0.980	0
	7	----	----	0
8		64.1	0.985	0
	8	----	----	0
9		72.5	0.995	1
	9	77.7	1.001	2
10		82.4	1.003	1
	10	86.6	1.003	2
11		89.5	1.008	1
	11	95.8	0.995	1
12		99.9	1.008	1
	12	105.6	1.006	1

AVERAGE

1.002

SCALE FACTOR

AVERAGE DEVIATION

0.0057

TABLE V

Structure of Trifluoromethylacetylene, $\text{CF}_3\text{C}'\text{C}''\text{H}$, C_{3v}

Parameter	Value	Limits of Error
CF	1.335\AA°	0.01\AA°
CC'	1.464\AA°	0.02\AA°
C'C''	1.201\AA°	0.002\AA°
C''H	1.056\AA°	0.005\AA°
FCF Angle	107.5°	1.0°

The significance of these values of the parameters is discussed after the presentation of the values of the parameters of perfluorobutyne-2 in Section I.C of this thesis.

The interrelation of electron diffraction and microwave data may be expressed in terms of the intersection of a geometric surface which defines limits of error for electron diffraction in the N -dimensional parameter space with the sheet of $(N - n)$ dimensions which approximately represents the freedom remaining in the choice of parameters when n moments of inertia are known from the microwave spectrum. On this microwave sheet, limits based on more general knowledge of molecular structures may be drawn; these limits are equally available for the electron diffraction determination. In the ideal case, the model in best agreement with the electron diffraction data lies on the microwave sheet and at the center of the electron diffraction limiting surface.

The advantage accruing from the use of electron diffraction data is the reduction of limits based on a general knowledge of molecular structure to diffraction limits of error; the advantages accruing from the use of microwave data are the usually very great limitation of the position of the model with respect to certain directions in parameter space, including often some corresponding to the positions of atoms which do not scatter electrons strongly. The most

valuable sort of combination is one which minimizes the area of the microwave sheet included by the diffraction limit-of-error surface and the fraction of the volume of this limit-of-error surface which is allowed by the microwave sheet. For particular arbitrary parameters the total range of allowed variation may be minimized under circumstances which do not correspond to this criterion. In any case, the situation for a certain molecule will not be a matter of choice unless the possibility of using only some of the accessible isotopic species is under consideration.

In trifluoromethylacetylene there is a fortunate combination of methods. Two parameters of direct interest, $C'^{1}H$ and $C'C''$, neither one well determined by electron diffraction, are accurately determined by the microwave data, and the fifth, the sole remaining one, is easily found from electron diffraction.

C. Perfluorobutyne-2

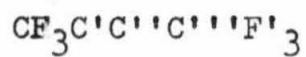
Perfluorobutyne-2 is of interest for reasons similar to those given for the study of trifluoromethylacetylene. The sample of the butyne (heat of vaporization and extrapolated B.P. from vapor pressure-temperature measurements, 4840 cal/mole and -24° ; lit⁽¹²⁾ B.P., -24.6°) was furnished by Professor Albert L. Henne of the Ohio State University. The possible presence of an impurity, perhaps perfluoromethylallene⁽¹²⁾, was neglected in the interpretation of

the diffraction pattern. Sample bulb temperatures were from -51° to -70° ; the electron wavelength was 0.06040\AA and the camera distance was 10.98 cm.

The values of the relative temperature factor coefficients are given in Table VI; they were chosen in general, to be consistent with those used for trifluoromethylacetylene. The values were roughly confirmed, as for the propyne, by approximate calculation of mean square displacements on assumption of the simple valence potential function and reasonable vibrational frequency values. The effects upon the $C''F$ and FF' mean square displacements of bending of the carbon axis were estimated by a separate treatment of X_2Y_2 ($D_{\infty h}$) with X equals C and Y equals CF_3 , that is, with the assumption that the vibrational frequencies characteristic of the CF_3 -groups (including the bending of CF_3 as a whole against the adjacent CC) are high enough relative to the low frequency bending of the carbon axis that the CF_3 -groups may be treated as rigid. (The bending force constant about the acetylenic carbons was taken to be the same as for methylacetylene. The lower bending frequency is then about 125 cm^{-1} , while in the propyne the frequency was observed to be about 170 cm^{-1} (10).) In principle an instrumental temperature factor coefficient (of the form $\frac{m^2 r_{ij}^2}{2 L^2}$, where m is the root mean square radius of the jet of gas as it exists in the diffraction region, r_{ij} is the interatomic

TABLE VI

Relative Temperature Factor Coefficients, Perfluorobutyne-2,



Atom Pair	$a_{ij} \times 10^4$
CF	0.2
C'F	0.8
C''F	3.1
C'''F	5.1
FF	0.6
CC'	0.1
CC''	0.5
C'C''	0.0
CC'''	0.9
FF'	29.0

distance to which this instrumental temperature factor coefficient is to be applied, and L is the camera distance) has been added to the real vibrational contribution, and, indeed, the value for FF' (Table VI), which otherwise is too big, can be accounted for by a reasonable m (about 1 mm). Some a_{ij} 's are not quite consistent but were not readjusted. The value of $a_{FF'}$ was also tested to some extent by calculation of curves for a range of values.

The root mean square angular displacement from linearity about each acetylenic carbon is, according to the X_2Y_2 approximation, 9.5° . Numerical calculation of the difference in the rigid-model distance $C'''F$ and the average value of this distance leads to a shortening of almost 0.01\AA . This slight shortening affects the diffraction pattern appreciably. The shortening of the FF' distances is unimportant in the interpretation of the diffraction pattern and has been neglected.

The solid-line visual intensity curve of Figure 2 was drawn from the photographs of the butyne by comparison with the photographs and the theoretical intensity curve $107.5^\circ B$ of the propyne. From it the radial distribution curve was calculated. The dashed additions to the visual curve represent the independent impressions of Professor Schomaker.

About 175 theoretical intensity curves were calculated with the omission of FF' terms and with the CF distance held constant at 1.33 for values of FF from 2.11 to 2.17,

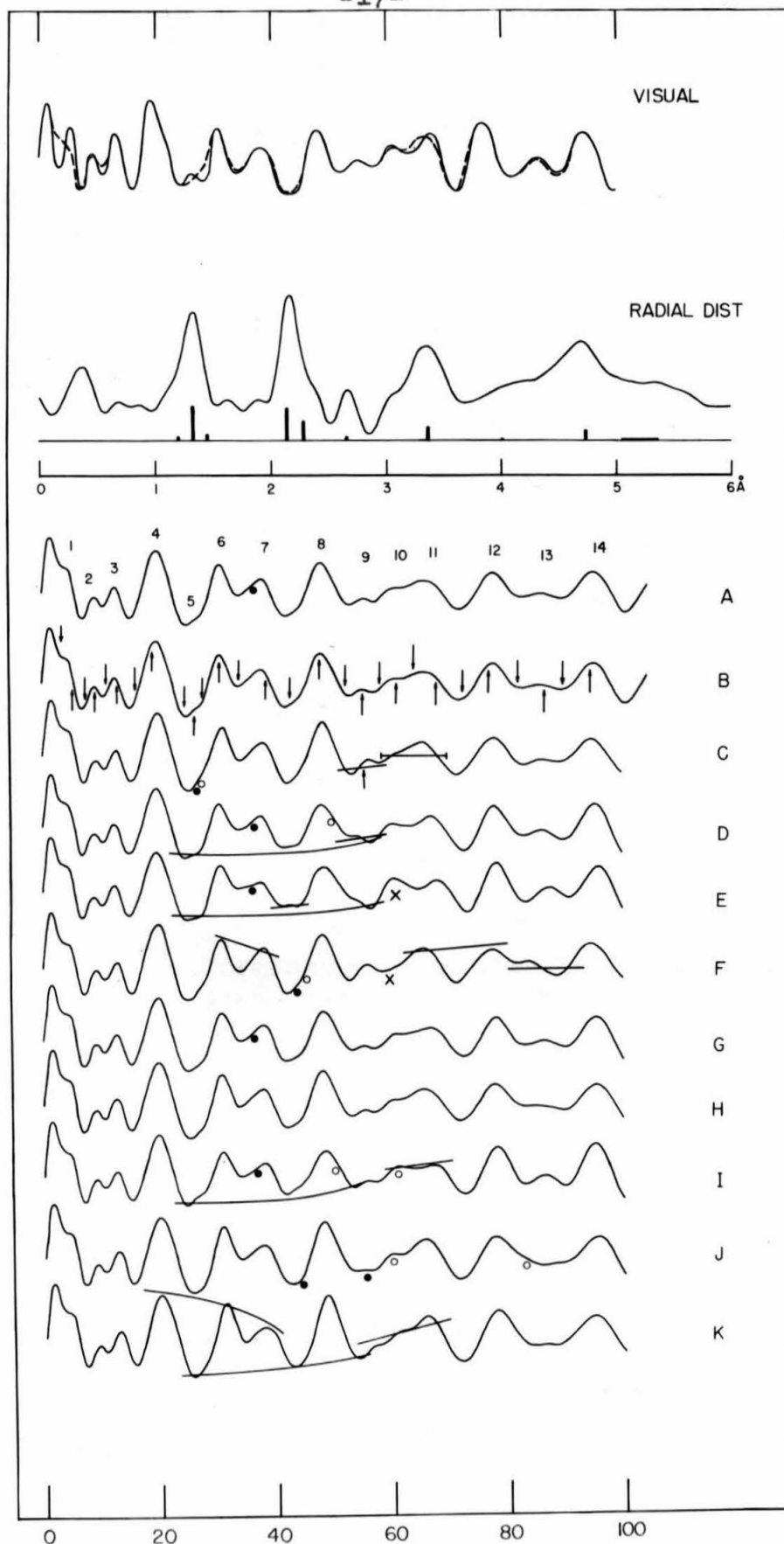


Figure 2. Perfluorobutyne-2

TABLE I

Explanation of Critical Marks of Figure 2.

Curve	Position	Mark	Meaning
A	7 max	Black dot	Inner slope should be more convex upwards. Creation operator.
B	All max, all min	Arrows	Position of maxima and minima as measured from photographs, corrected by scale factor. Best curve.
C	5 max	Black dot White dot	5 max should be found farther downwards and to the left. White dot is destruction operator.
C	9 min, 10 min	Line	9 min is too deep; 10 min, too shallow. Depths should be as line indicates.
C	9 max	Arrow	9 max is significantly misplaced relative to adjacent features. The arrow is the same as the one shown on the best curve.
C	10 max, 11 max	Terminated line	Feature should be wider, with approximate width as indicated.
D	5 min- 9 min	Curved line	8 min should lie below a line from 5 min to 9 min with relative depths as indicated.
E	8 min	Line	Feature in bottom of 8 min should lie closer to 8 max than to 7 max.
E	10 max	Cross	Completely unacceptable feature; compare standard.
F	6 max, 7 max	Line	7 max is too high relative to 6 max. Line indicates desired heights.
F	13 max	Line	13 max should lie between minima of almost equal depth.
K	4 max- 7 max	Curved line	6 max too high relative to 4 max and 7 max. Heights should lie along curve.
K	9 max- 11 max	Line	Region should slope upwards more gently.

CC' from 1.35 to 1.51, and C'C'' from 1.14 to 1.29. In all models, D_3 symmetry was assumed, and when FF' terms were finally added free rotation of the CF_3 -groups was assumed. The parameters of a few of these models are presented in Table VII, and the intensity curves, including FF' terms, are reproduced in Figure 2.

A limit-of-error surface in shape-parameter space was established by detailed consideration of all the theoretical curves; the positions of the illustrated models relative to this surface are indicated in Table VII. Curve K is a fairly good curve, the best in its own isolated region, but is regarded as unacceptable. Several attempts to find acceptable models in which the C'F and FF distances are interchanged were unsuccessful and unpromising.

The determination of the scale factor for Model B is presented in Table VIII; the complete structure, in Table IX.

The dimensions of the CF_3 -groups in trifluoromethylacetylene and perfluorobutyne-2 are the same as those in 1,1,1-trifluoroethane and perfluoroethane⁽⁹⁾. Methylacetylene⁽¹³⁾, with HCH angle of $108^\circ 14'$ and CC' of 1.460\AA , shows the same sort of abnormalities as the fluorinated alkynes. The length of the triple bond is quite insensitive to the electronegativity of the substituents on the methyl group. It seems likely that the triple bond is dominant in the determination of the adjacent C-C distance and the methyl-group bond angles. Accordingly, the FCF angle of 107.5° may satisfy simultaneously the requirements

TABLE VII

Parameters of Theoretical Intensity Curves, Perfluorobutyne-2

Model**	FF	CC'	C'C''	Scale Factor (CF equals 1.33)
A*	2.15	1.46	1.21	1.007
B*	2.15	1.46	1.21	1.006
C#	2.15	1.43	1.20	1.009
D	2.15	1.49	1.20	1.008
E	2.13	1.47	1.20	1.013
F	2.17	1.47	1.20	1.000
G*	2.15	1.47	1.20	1.008
H*	2.15	1.45	1.23	1.004
I#	2.15	1.49	1.14	1.011
J#	2.15	1.43	1.29	1.008
K	2.13	1.37	1.26	1.013

* Models marked with an asterisk (*) are within the acceptable region of parameter space; those marked with the symbol (#) are near the boundaries of the acceptable region, either within or without ; those unmarked are far outside.

** Account of apparent shortening of CC''' and C'''F through bending of the carbon axis is taken in Model B.

TABLE VIII

Scale Factor, Perfluorobutyne-2

Min	Max	q_{obs}	$q_{calc}/q_{obs}(B)$	Weights	
				I	II
1		3.4	1.014	0	0
	1	5.4	0.852	0	0
2		7.5	0.935	1	0
	2	9.1	0.998	1	0
3		11.0	0.952	1	0
	3	12.8	0.966	1	0
4		16.0	0.945	1	0
	4	19.04	1.035	1	2
5		24.6	1.018	0	0
	5	26.2	1.006	0	0
6		27.5	0.991	0	0
	6	30.5	1.000	1	0
7		33.78	1.004	1	1
	7	38.3	0.986	1	0
8		42.5	0.985	0	0
	8	47.62	1.008	1	5
9		52.1	1.019	1	0
	9	55.14	1.003	1	3
10		58.0	0.987	1	0
	10	60.9	0.998	1	0
11		63.9	0.978	1	0
	11	67.6	0.975	1	0
12		72.26	0.996	1	4
	12	76.66	1.016	1	4
13		81.8	1.014	1	0
	13	86.36	0.991	1	4
14		89.6	1.004	1	0
	14	94.24	1.011	1	2

AVERAGE I 0.992

AVERAGE DEVIATION I 0.019

AVERAGE II 1.006

SCALE FACTOR

AVERAGE DEVIATION II 0.009

TABLE IX

Structure of Perfluorobutyne-2

Parameter	Value	Limits of Error
CF	1.340 ^o Å	0.020 ^o Å#
CC'	1.465 ^o Å	0.055 ^o Å*#
C'C''	1.22 ^o Å	0.09 ^o Å#
FCF Angle	107.5 ^o	1.0 ^o

* If C'C'' is assumed to be 1.22^oÅ, then the limit of error is 0.040Å for CC' and is unchanged for the other parameters.

Including \pm 1.0% estimated limit of scale error.

of a stable CF_3 -group and the requirements of the most stable carbon skeleton.

The smaller-than-tetrahedral FCF angle is indicative of extra p-character in the CF bonds and extra s-character in the CC' bond. The shortening of CC' seems to depend somewhat on this extra s-character of the C orbital as well as on double-bond character through conjugation, on s-character of the C' orbital with perhaps a shortening of $0.03\overset{\text{O}}{\text{\AA}}$ as for acetylenic CH bonds, on extra s-character of the C orbital because of double-bond formation to the fluorines, and on a shortening of the C radius because of the loss of electrons to the fluorine atoms. On the other hand, the CF distance should be affected by double-bond formation, extra p-character of the sigma bond orbitals, and a correction for the ionic character of C.

Of the many possible detailed explanations of the structure and dipole moment of trifluoromethylacetylene, the following is proposed in which shortening of bonds is accounted for only by double-bond formation and extra s-character. If C' is assumed to be neutral, if CC' is shortened through extra s-character by $0.03\overset{\text{O}}{\text{\AA}}$, if the double-bond character of CC' (18%) as then deduced from the bond length measures the contribution of structures in which C'' or H has a positive formal charge and C is neutral, and if the difference of charges of H and C'' remains 0.16 electrons, corresponding to 8% ionic character for an uncharged C-H group, then use of the observed⁽¹⁰⁾ dipole moment of 2.36

Debye indicates that the CF bonds have about 13% net ionic character. Simultaneous solution for the effective difference in electronegativity of C and F and for the bond order n of the CF bond (through the use of the Schomaker-Stevenson Rule⁽¹⁴⁾ corrected for bond order by $0.700 \log n$ and through the use of the relation of ionic character to electronegativity difference) leads to the values 1.3 and 1.20 respectively. The ionic character of the CF σ -bond is then 33%. The net charges on F, C, C'', and H are 0.13, -0.32, 0.04, and -0.12 electrons respectively.

D. Tetramethylsilane

At the suggestion of Professor Schomaker a redetermination of the SiC distance in tetramethylsilane, $\text{Si}(\text{CH}_3)_4$, was undertaken to determine whether this SiC distance was really an exception to the Schomaker-Stevenson Rule⁽¹⁴⁾ that

$$r_{AB} = r_A + r_B - 0.09 |x_A - x_B|,$$

in view of the fact that the SiC single bond in this compound has been reported⁽¹⁵⁾ to be $1.93 \pm 0.03 \text{ \AA}$ instead of 1.88 \AA to 1.90 \AA as found⁽¹⁶⁾ in carborundum, and 1.88 \AA as predicted by the Rule. The value 1.87 \AA has recently been reported⁽¹⁷⁾ in the three other methylsilanes and the SiC distance in $\text{Si}_2(\text{CH}_3)_6$ is⁽¹⁸⁾ $1.90 \pm 0.02 \text{ \AA}$.

Tetramethylsilane was prepared by the addition at about 40° of silicon tetrachloride dissolved in *n*-butyl ether to excess methyl magnesium iodide prepared in *n*-butyl

ether. The mixture was refluxed at about 60° for nine hours under a 62-cm water-cooled reflux condenser maintained at less than 10° . After the volatile products which passed the condenser to a trap cooled with a dry ice-acetone mixture were returned to the Grignard solution, heating was continued for five hours at about 90° with the condenser at less than 10° , and then for a short time, still collecting the volatile material in the dry ice-acetone trap, with the condenser at about 26° .

The product, which contained impurities less volatile than tetramethylsilane, was fractionally distilled in a 20-cm Vigreux column of an unknown number of plates at a reflux ratio of about 20. A middle fraction, about 3 cc, had a vapor pressure of 264.1 mm at 0.00° . If trimethylchlorosilane was the sole impurity, this distillate was about 96% pure tetramethylsilane.

Sample bulb temperatures ranged from -17° to -43° . The electron wavelength was 0.06059\AA ; the camera distance, 10.94cm.

Theoretical intensity curves were calculated, with appropriate temperature factors, for SiC equal to 1.89, for SiH from 2.45 to 2.53, and for CH from 1.06 to 1.14. Both the opposed and staggered orientations of the methyl groups relative to the C_3Si framework were considered in all these models. In the estimation of the temperature factor coefficients for the rotation-dependent CH distances the height of the assumed three-fold-cosinusoidal potential barrier was taken to be 1.3 k cal/mole⁽¹⁹⁾. An effective value, 1.25, was used for Z_{H} . All HH interactions were

neglected. A good fit to the qualitative features of the visual intensity curve was obtained for angle SiCH equal to 110° , and CH equal to 1.10. A model in which most, but not all, of the methyl groups are staggered relative to C_3Si is to be preferred on the basis of the qualitative features of the pattern as well as the quantitative comparisons summarized in Table X. The final results are: angle SiCH, $110^\circ \pm 3^\circ$; CH, $1.10 \pm 0.05\text{\AA}$; and SiC, $1.888 \pm 0.02\text{\AA}$ (estimated limit of scale error, $\pm 0.8\%$). This, in confirmation of the Schomaker-Stevenson Rule.

E. Tungsten Hexacarbonyl

Interest in tungsten hexacarbonyl, $W(CO)_6$, rose from the difficulties in completing satisfactorily the structure of molybdenum hexacarbonyl, the structure of which was undertaken at the suggestion of Professor Pauling. A study⁽²⁰⁾ of the structure of $W(CO)_6$ based on electron diffraction data for values of q less than about 44 yielded a WC distance of $2.06 \pm 0.04\text{\AA}$ and a CO distance of $1.13 \pm 0.05\text{\AA}$, with octahedral symmetry assumed. An x-ray study⁽²¹⁾ of the crystals merely placed an upper limit of 2.3\AA upon the WC distance.

The sample of $W(CO)_6$ was obtained from A. D. Mackay, Inc., of New York City. Pictures were taken at temperatures from 97° to 109° with a sample bulb of about 40 cc capacity. Although the compound decomposes readily above about 107° , excellent photographs of undecomposed $W(CO)_6$ with scattering

TABLE X

Scale Factor, Tetramethylsilane

Min	Max	q _{obs}	q _{calc} /q _{obs}		Weights	
			Opposed*	Staggered*	I	II
	1	7.9	0.954	0.992	0	0
2		10.8	0.869	0.939	0	0
	2	14.1	0.916	0.980	0	0
3		18.1	1.015	0.985	1	0
	3	20.8	1.100	1.021	1	0
4		23.2	1.056	0.995	1	0
	4	25.4	1.029	0.988	1	0
5		30.02	1.001	0.996	1	1
	5	33.85	1.012	1.018	1	1
6		38.6	0.998	0.998	1	0
	6	45.4	0.985	0.992	1	0
7		50.56	0.993	0.992	1	1
	7	55.20	1.007	1.009	1	1
8		61.31	1.003	1.003	1	1
	8	65.92	1.001	1.001	1	1
9		71.65	0.992	0.991	1	1
	9	77.00	0.997	0.997	1	1
10		82.50	0.997	0.997	1	1
	10	87.93	0.993	0.993	1	1
11		92.91	0.996	0.996	1	1
	11	98.36	0.995	0.995	1	0
AVERAGE I			1.009	0.998		
AVERAGE DEVIATION I			0.018	0.011		
AVERAGE II			0.999	0.999	SCALE FACTOR	
AVERAGE DEVIATION II			0.005	0.006		

* T_d models: CH, 1.10Å; angle SiCH, 110°.

to the limit of the camera were obtained with less difficulty than for Mo(CO)_6 . The electron wavelength was 0.06075\AA ; the camera distance, 10.94 cm.

The gross appearance of the photographs as well as the radial distribution curve made from visual I of Figure 3 indicate that there exist at least two different WC and at least two different WO distances. Visual II, by Professor Schomaker, confirms these observations. The standard curve was considered to be a combination of visual I and visual II with considerably more weight given to the latter.

Theoretical intensity curves were calculated for the entire plausible range of the six independent parameters described in Table XI for models containing three long and three short WC bonds, with, however, only the WC, WO, and bonded CO terms included in most cases. The parameters of 33 of the total of 179 models for which curves were calculated are reproduced in Table XII and their intensity curves are presented in Figures 3, 4, 5, and 6. The first letter in a curve designation indicates the set of relative temperature factor coefficients used (Table XIII), and the letter Z indicates that account has been taken of the variation in scattering power of C and O relative to W as a function of q . For the curves without a letter Z an effective value, 65, was used for Z_W . Badger's Rule⁽²²⁾ and reasonable bending frequencies were used with the assumption of the simple valence potential function to estimate the values of the relative temperature factor coefficients.

TABLE XI

Definition of Parameters, Tungsten Hexacarbonyl

Parameter	3:3 Split	2:4 Split*
Long CO	$a = a' + m$	$a = \frac{a' + a''}{2} + u$
Mean CO (SCALE)	$s = \frac{a + a'}{2}$	$s = \frac{a + a' + a''}{3}$
Short CO	a'	a'
Short CO	----	$a'' = a' - v$
Short WC	b	b
Long WC	$b' = b + n$	b'
Long WC	----	$b'' = b' + w$
Short WO	$c = a + b - u$	$c = a + b$
Long WO	$c' = a' + b' - u'$	$c' = a' + b'$
Long WO	----	$c'' = a'' + b''$

* u, v, and w are greater than or equal to zero; u is greater than v.

TABLE XII

Values of Parameters, Tungsten Hexacarbonyl

Model**	S	m	b	n	u	u'	Scale Factor
1*	1.13	0.00	1.95	0.23	0.00	0.00	(Table XIV)
2*	1.15	0.04	1.95	0.27	0.00	0.00	(Table XIV)
3#	1.15	0.06	1.95	0.27	0.02	0.00	----
5#	1.13	0.00	1.93	0.23	0.00	0.00	0.994
6*	1.13	0.00	1.93	0.25	0.00	0.00	1.006
7#	1.13	0.00	1.95	0.25	0.00	0.00	0.999
8	1.13	0.00	1.97	0.21	0.00	0.00	0.998
9	1.15	0.04	1.93	0.25	0.00	0.00	1.003
10#	1.15	0.04	1.93	0.29	0.00	0.00	0.994
11*	1.15	0.04	1.97	0.25	0.00	0.00	0.987
12#	1.15	0.06	1.95	0.25	0.00	0.00	0.996
13*	1.15	0.06	1.95	0.27	0.00	0.00	0.992
14	1.15	0.06	1.99	0.27	0.00	0.00	0.976
15	1.15	0.10	1.97	0.29	0.00	0.00	0.980
16*	1.13	0.00	1.93	0.23	0.02	0.00	----
17	1.13	0.00	1.89	0.23	0.06	0.00	1.032
18#	1.13	0.00	1.91	0.23	0.00	0.02	----
19*	1.13	0.00	1.93	0.25	0.00	0.02	1.008
20#	1.13	0.00	1.95	0.23	0.00	0.02	----
21*	1.13	0.00	1.91	0.23	0.02	0.02	----
22#	1.13	0.00	1.87	0.21	0.06	0.04	----
23#	1.13	0.00	1.89	0.27	0.00	0.06	1.024
24#	1.13	0.00	1.83	0.25	0.04	0.06	1.056
25*	1.15	0.06	1.95	0.23	0.04	0.00	----
26#	1.15	0.06	1.91	0.23	0.06	0.00	----
27	1.15	0.06	1.91	0.27	0.06	0.00	----
28#	1.15	0.06	1.95	0.23	0.06	0.00	----
29	1.15	0.06	1.89	0.21	0.10	0.00	1.035
30#	1.15	0.06	1.95	0.27	0.00	0.02	0.994
31#	1.15	0.06	1.87	0.25	0.06	0.04	1.037
32#	1.15	0.10	1.91	0.27	0.06	0.00	1.013
33	1.15	0.10	1.89	0.23	0.10	0.00	1.031
34	1.15	0.10	1.85	0.27	0.06	0.04	1.042

** C_{3v} except for model 4, which has the following values of parameters: S, 1.15; u, 0.03; v, 0.00; w, 0.10; b, 1.98; b', 2.20.

* Models marked with an asterisk (*) are within the acceptable region of parameter space; those marked with the symbol (#) are near the boundaries, either within or without; those unmarked are far outside.

TABLE XIII

Relative Temperature Factor Coefficients, Tungsten Hexa-
carbonyl

Distance*	$a_{ij} \times 10^4$				
	A	B	C	D	E
Long CO	0.0	0.0	0.1	0.0	0.1
Short CO	0.0	0.0	0.0	0.0	0.0
Short WC	0.5	0.5	0.5	0.5	0.5
Long WC	0.8	0.8	0.8	0.8	0.8
Short WO	1.2	1.2	1.2	1.2	1.2
Long WO	1.4	1.4	1.4	1.4	1.4
Opposite CC	3.6	1.9	1.9	---	---
Opposite CO	5.4	2.6	2.6	---	---
Opposite OO	7.3	3.2	3.2	---	---
Adjacent CC	3.8	3.0	3.0	---	---
Adjacent CO	5.3	3.8	3.8	---	---
Adjacent OO	7.2	4.9	4.9	---	---

* Distances which lack values of a_{ij} were omitted from models.

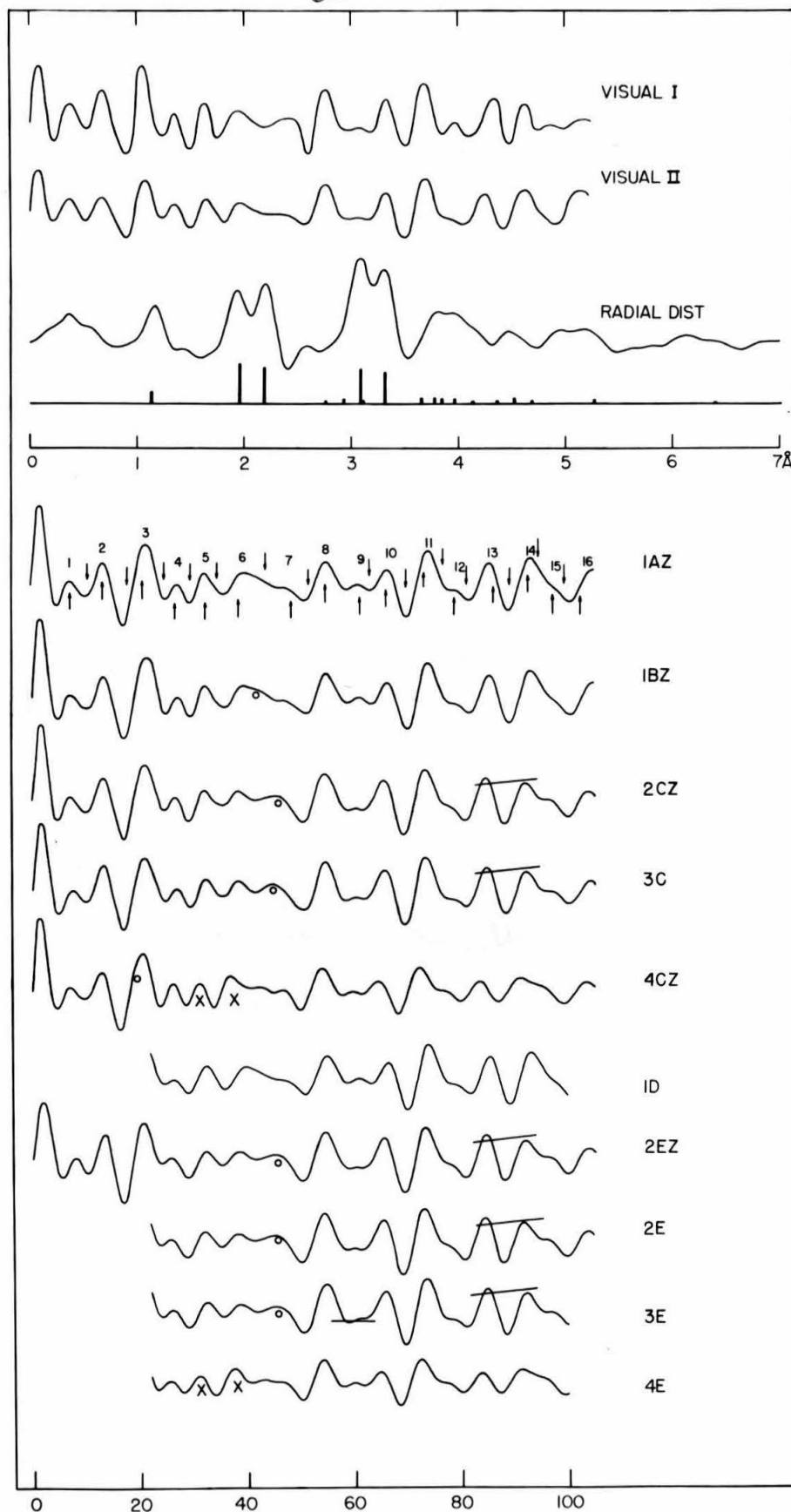


Figure 3. Tungsten Hexacarbonyl

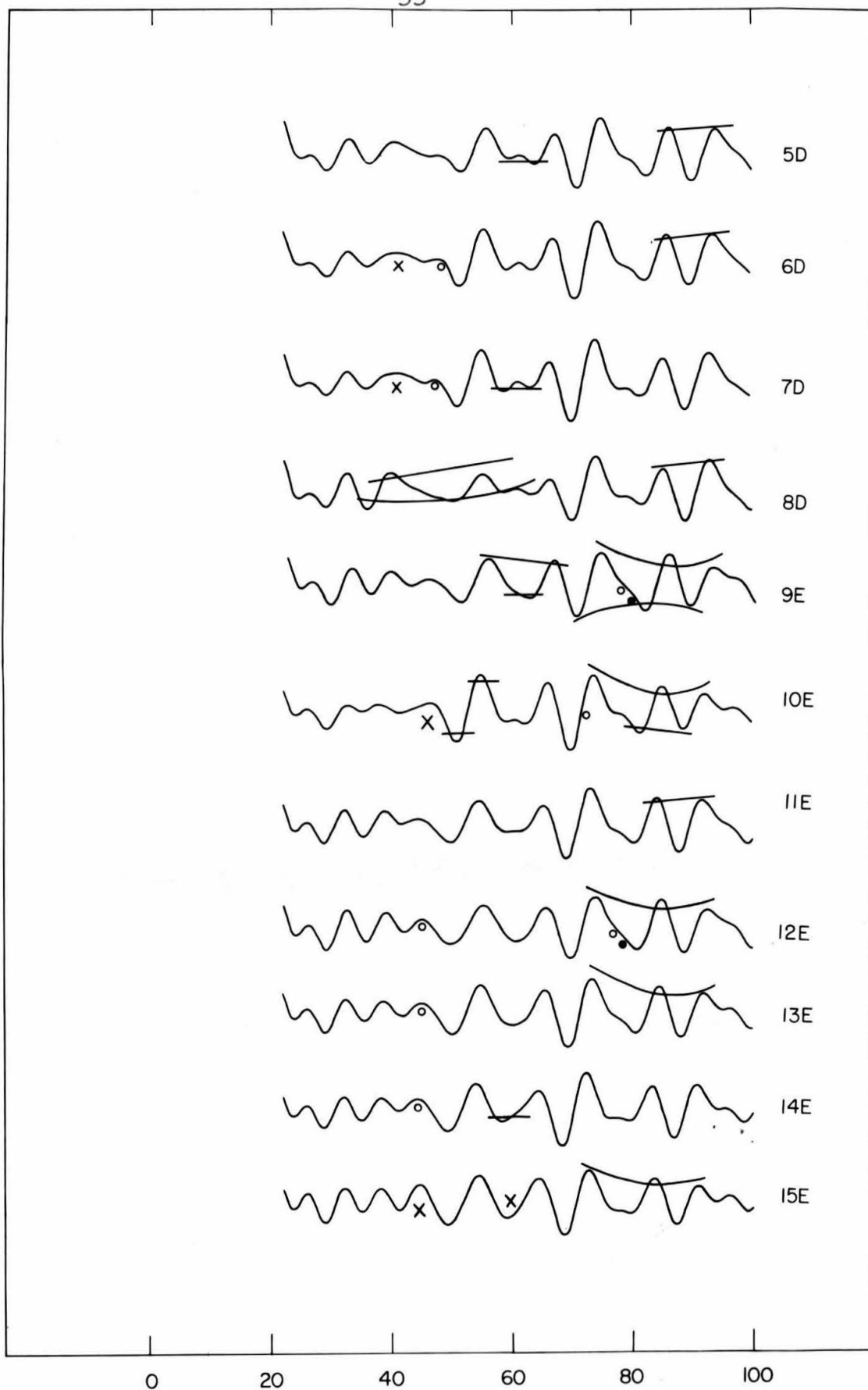


Figure 4. Tungsten Hexacarbonyl

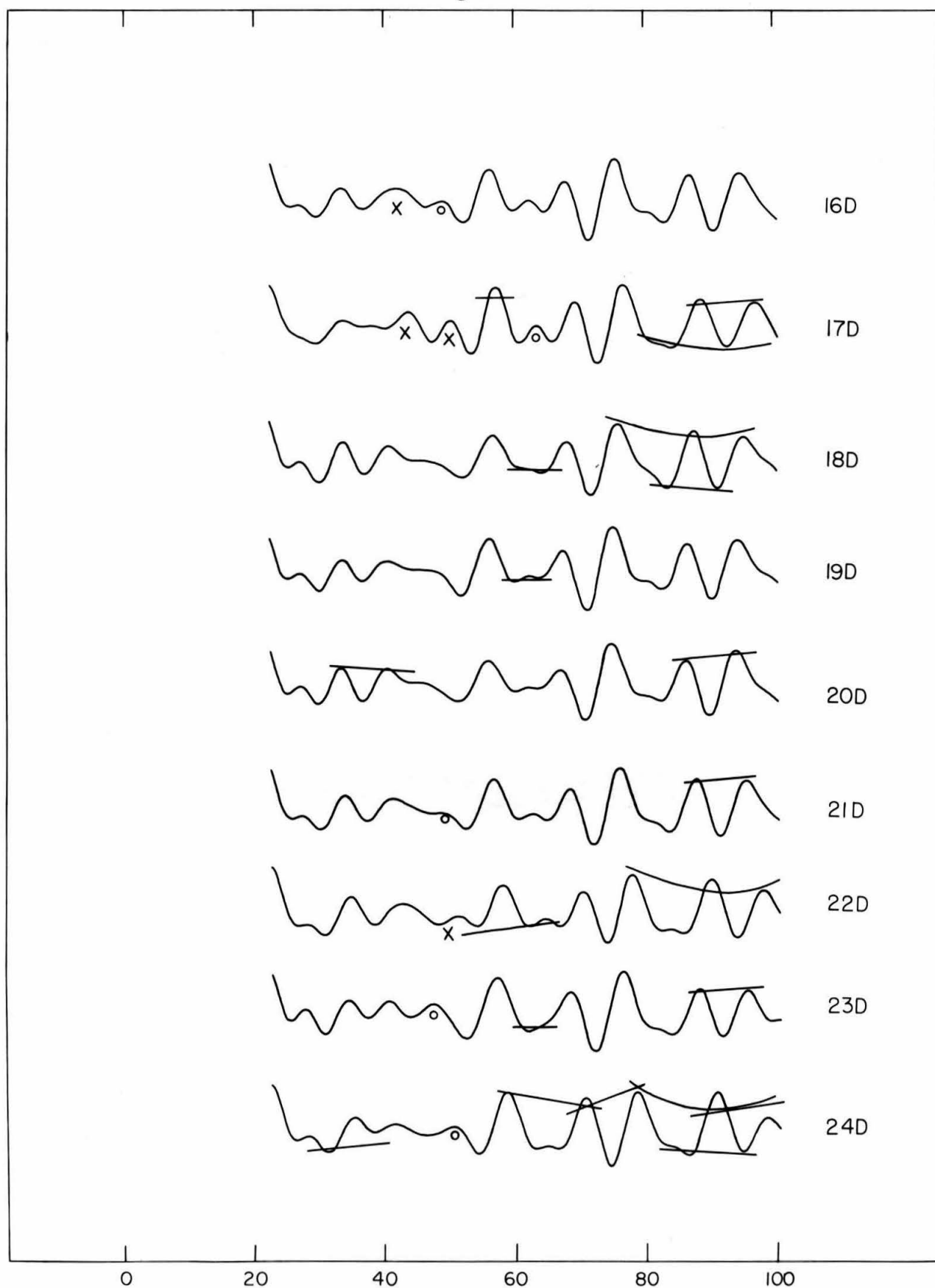


Figure 5. Tungsten Hexacarbonyl

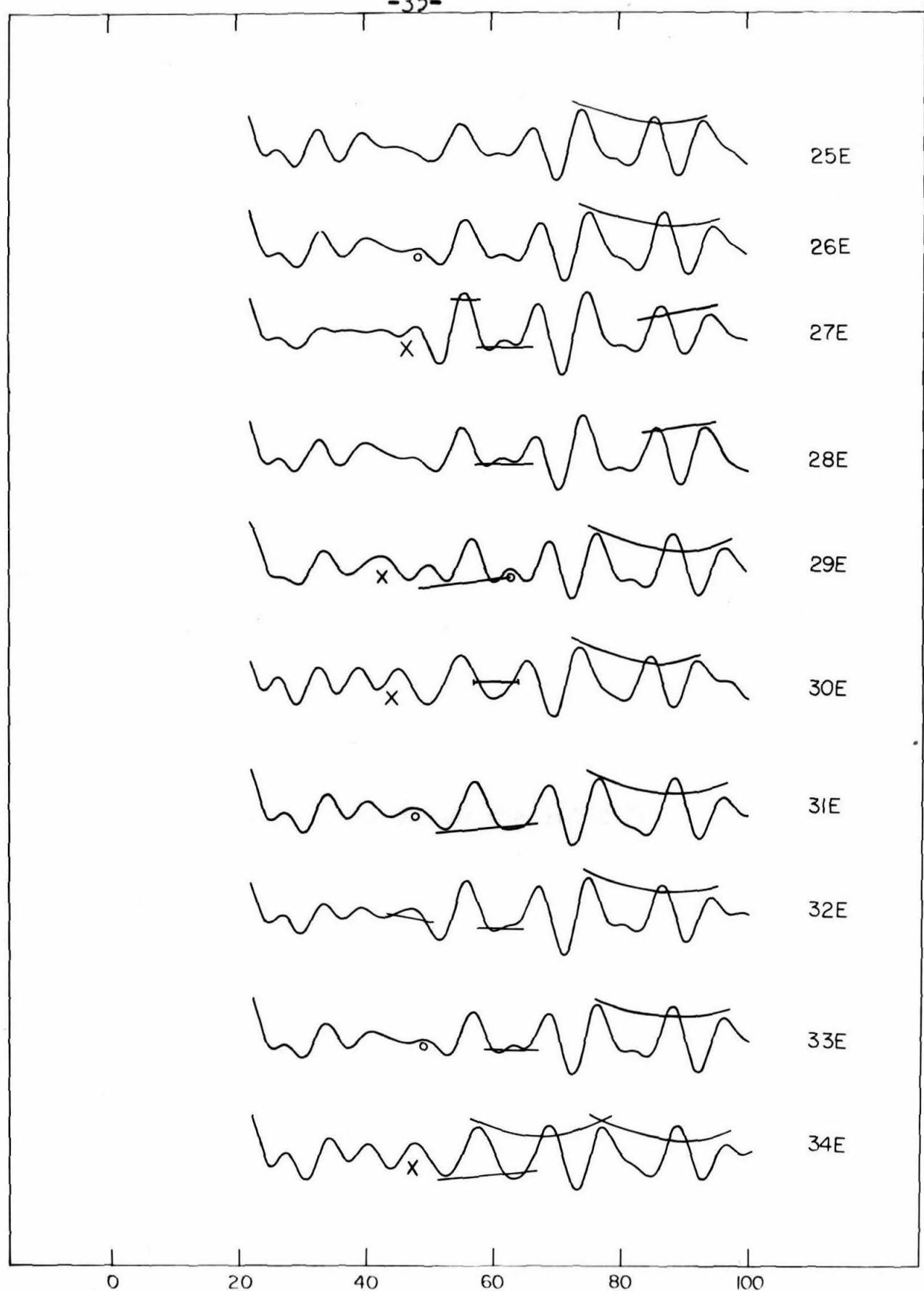


Figure 6. Tungsten Hexacarbonyl

Curves 1AZ, 1BZ, and 2CZ, each for CWC angles of 90° , are considered to be more satisfactory than any of the other models because they involve a minimum of variable parameters, the general quality of fit not being improved by consideration of non-linear WCO-groups or by adjustment, as in 3C (angle short CWC, 105° ; angle long CWC, 84°), of all eight parameters of the C_{3v} -structure.

Curve 4E, the best of 67 curves calculated for various values of the six parameters of Table XI for two short and four long WC, is unsatisfactory. Moreover, model 4 cannot be rendered acceptable by the addition of the neglected CC, CO, and OO scattering terms even for CWC angles varying widely from 90° , the value used in 4CZ. Less than about two and one-half short WC and more than about three and one-half long WC cannot constitute the structure of $W(CO)_6$. This last conclusion is subject to some extent, of course, to the restrictions of Table XI on the 2:4 models.

The final results are given in Table XV, in the derivation of which incomplete curves (e.g., 5D, 10E, etc.) were used except for the best models of cases A and B. The scale factor for case A is based on curve 1AZ (Table XIV) and that for case B on a combination of 1AZ and 2CZ. An interpretation of the structure is given in Section II of this thesis.

TABLE XIV

Scale Factor, Tungsten Hexacarbonyl

Min	Max	q_{obs}	$q_{\text{calc}}/q_{\text{obs}}(1\text{AZ})$	$q_{\text{calc}}/q_{\text{obs}}(2\text{CZ})$	Weights	
					I	II
	1	7.3	0.981	0.967	0	0
2		10.5	0.963	0.953	0	0
	2	13.3	1.006	0.987	0	0
3		18.0	0.949	0.952	0	0
	3	20.8	1.029	1.010	2	0
4		24.8	1.011	0.991	1	0
	4	26.9	1.012	0.993	2	0
5		29.8	0.995	0.982	1	0
	5	32.5	0.993	0.985	1	0
6		34.8	1.036	1.022	1	0
	6	38.8	1.027	0.992	1	0
7		43.7	-----	0.953	0	0
	7	48.6	0.986	0.955	0	0
8		51.8	0.986	0.975	1	0
	8	54.99	1.001	0.992	2	1
9		-----	-----	-----	0	0
	9	61.50	0.993	0.985	2	1
10		63.4	0.999	0.975	1	0
	10	66.39	1.002	0.990	2	1
11		69.94	1.002	0.992	2	2
	11	73.46	1.009	1.000	2	1
12		76.9	1.013	0.999	1	0
	12	79.1	1.009	0.996	1	0
13		81.4	1.005	0.995	1	0
	13	86.4	0.990	0.979	1	0
14		89.46	0.997	0.985	2	1
	14	92.8	1.005	0.992	1	0
15		94.7	1.020	1.005	1	0
	15	97.5	1.010	0.995	1	0
16		99.6	1.009	1.004	1	0
	16	102.7	1.022	1.011	0	0
17		(105.1)	-----	-----	0	0
	17	(109.0)	-----	-----	0	0
AVERAGE I			1.006	0.993		
AVERAGE DEVIATION I			0.009	0.007		
AVERAGE II			1.001	0.991	SCALE FACTOR	
AVERAGE DEVIATION II			0.003	0.004		

TABLE XV

The C_{3v} Structure of Tungsten Hexacarbonyl on Several Assumptions Regarding CO Split and WCO Angle

Parameter	A	B	C
Mean CO	$1.131 \pm 0.02 \text{ \AA}$	$1.133 \pm 0.02 \text{ \AA}$	$(1.10 \text{ \AA} - 1.21 \text{ \AA})$
Split, CO	$0.000 \text{ \AA} *$	0.010 \AA $(0.000 \text{ \AA} - 0.075 \text{ \AA})$	$(0.00 \text{ \AA} - 0.10 \text{ \AA})$
Short WC	$1.952 \pm 0.04 \text{ \AA}$	$1.947 \pm 0.04 \text{ \AA}$	$(1.90 \text{ \AA} - 1.99 \text{ \AA})$
Split, WC	$0.230 \pm 0.03 \text{ \AA}$	0.238 \AA $(0.210 \text{ \AA} - 0.282 \text{ \AA})$	$(0.210 \text{ \AA} - 0.285 \text{ \AA})$
Long WC	$2.182 \pm 0.04 \text{ \AA}$	$2.185 \pm 0.04 \text{ \AA}$	$(2.14 \text{ \AA} - 2.23 \text{ \AA})$
Angle WCO	$180^\circ *$	$180^\circ *$	$(155^\circ - 180^\circ)$

* Assumed.

Limits include $\pm 0.5\%$ estimated limit of scale error.

F. Molybdenum Hexacarbonyl

At the suggestion of Professor Pauling, redetermination of the structure of molybdenum hexacarbonyl, $\text{Mo}(\text{CO})_6$, was undertaken. It had been reported⁽²⁰⁾ to be octahedral, with MoC equal to $2.08 \pm 0.04 \text{ \AA}$ and CO equal to $1.13 \pm 0.05 \text{ \AA}$. Although the space group symmetry of the crystals imposes no restriction upon the symmetry of the molecule, regular octahedral symmetry, with MoC equal to 2.13 \AA and CO equal to about 1.15 \AA has been found⁽²¹⁾ to be compatible with the x-ray data.

A sample of the carbonyl was supplied by Professor Pauling. In all, 105 photographs were taken at a camera distance of 10.92 cm in efforts to obtain clearly visible MoC and MoO scattering beyond q equals 65. Various sample bulbs of volumes up to 40 cc and various heating devices were used in vain at temperatures from 90° to 112° . The ten photographs taken at a camera distance of about 5.1 cm in order to observe, if possible, the reinforcing region of scattering, which would occur at large q if this carbonyl were like $\text{W}(\text{CO})_6$, were no better. The electron wavelength was taken to be 0.06042 \AA throughout these experiments.

A superficial study of the dissociation of $\text{Mo}(\text{CO})_6$ at temperatures of about 130° indicated that the pressure of CO above excess solid $\text{Mo}(\text{CO})_6$ is less than about ten mm even after one hour at 112° , where the rapidly attained vapor pressure of the carbonyl is 81 mm. Since the sample bulb was heated up just before the taking of the photographs,

decomposition was minimized and was probably negligible at least for the first picture of each set of five. Yet from none of many experiments came a photograph which showed MoC and MoO scattering to be even one-fifth as important at about q equals 70 as the obvious CO scattering.

This extraordinary decrease of the MoC and MoO scattering relative to CO scattering might be attributed to a great amplitude of stretching of the MoC bond and correspondingly severe temperature factor coefficients, such as those of Set C, Table XVI. Both Badger's Rule⁽²²⁾ and Gordy's Rule⁽²³⁾, however, predict a WC force constant ten times as large as would correspond to Set C.

This extraordinary decrease of the MoC and MoO scattering relative to CO scattering might also be attributed to the existence of at least two different MoC distances as in $W(CO)_6$. Indeed, the actual appearance of the photographs, as indicated by the visual intensity curve of Figure 7, which was drawn for q values greater than 65 largely by Professor Schomaker but with measurements by the author, indicates that this is the true explanation. The radial distribution curve however, was calculated from the part of the curve for q less than 65 and, accordingly, does not resolve the MoC and MoO groups.

Parameters of several possible models are given in Table XVII and their theoretical intensity curves are presented in Figure 7. In all models MoCO was assumed to be linear, the split in CO to be absent, and all adjacent C-Mo-C angles to be right angles.

TABLE XVI

Relative Temperature Factor Coefficients,
Molybdenum Hexacarbonyl

Distance	$a_{ij} \times 10^4$			
	A	B	C	D*
Mean CO	0.0	0.0	0.0	0.0
Short MoC	0.6	0.6	8.1	0.4
Long MoC	0.7	0.7	8.1	0.7
Short MoO	1.1	1.1	8.7	0.9
Long MoO	1.3	1.3	8.7	1.2
Opposite CC	3.6	3.6	18.6	1.3 - 1.9
Opposite CO	5.4	5.4	20.4	1.9 - 2.5
Opposite OO	7.3	7.3	22.3	2.4 - 3.0
Adjacent CC	6.5	3.8	11.3	6.5
Adjacent CO	8.8	5.3	12.8	8.8
Adjacent OO	13.4	7.2	14.7	13.4

* Used only with the $Z_i Z_j$ approximation, with effective Z 's 33, 6, and 8 for Mo, C, and O.

TABLE XVII

Values of Parameters, Molybdenum Hexacarbonyl

Model	Symmetry	Short MoC	Long MoC	Mean CO	Scale Factor
1*	C _{3v}	1.97	2.10	1.13	1.013 (1AZS)
2#	C _{3v}	1.99	2.12	1.13	1.002 (2AZ)
3#	C _{3v}	1.95	2.08	1.13	1.017 (3AZ)
4#	C _{3v}	1.96	2.11	1.13	1.010 (4AZ)
5#	C _{3v}	1.98	2.09	1.13	1.010 (5AZ)
6	O _h	2.01	----	1.13	-----
7	O _h	2.04	----	1.13	-----
8	O _h	2.07	----	1.13	-----
9	D _{4h}	1.93 (2)	2.07 (4)	1.13	-----

* Models marked with an asterisk(*) are within the acceptable region of parameter space; those marked with the symbol (#) are near the boundaries, either within or without; those unmarked are far outside.

As for $W(CO)_6$, a letter after the model number indicates the set of relative temperature factor coefficients used from Table XVI, and a letter Z indicates that account has been taken of the variation of scattering power of Mo relative to C and O. The most noticeable effect of this correction for scattering power is slightly to weaken minimum 6 and maximum 8 relative to adjacent features. The temperature factor coefficients were estimated on the usual assumption of the simple valence potential function with the use of Badger's Rule⁽²²⁾ and reasonable bending frequencies.

Not only do the O_h models C fail to provide a good fit in several ways for moderate values of q , but a C_{3v} model (1AZ) with linear MoCO groups, 90° adjacent CMO angles, and reasonable temperature factors fits well everywhere except at maximum 8. This feature is probably in error in the visual curve. Curve 1AZS, which was calculated for a 0.01\AA shortening of MoO due to bending of angle MoCO and is actually a trifle less satisfactory at maximum 8 than 1AZ, illustrates the impossibility of obtaining improvement by assuming moderate MoO shortening such as might arise from the MoCO bending vibration and might possibly be compatible with the rest of the diffraction pattern.

Model 9 represents the best of nineteen D_{4h} models each calculated with D temperature factors. It appears that for $Mo(CO)_6$, as for $W(CO)_6$, the number of short metal-carbon bonds must be greater than about two and one-half and that the number of long metal-carbon bonds must be less than about

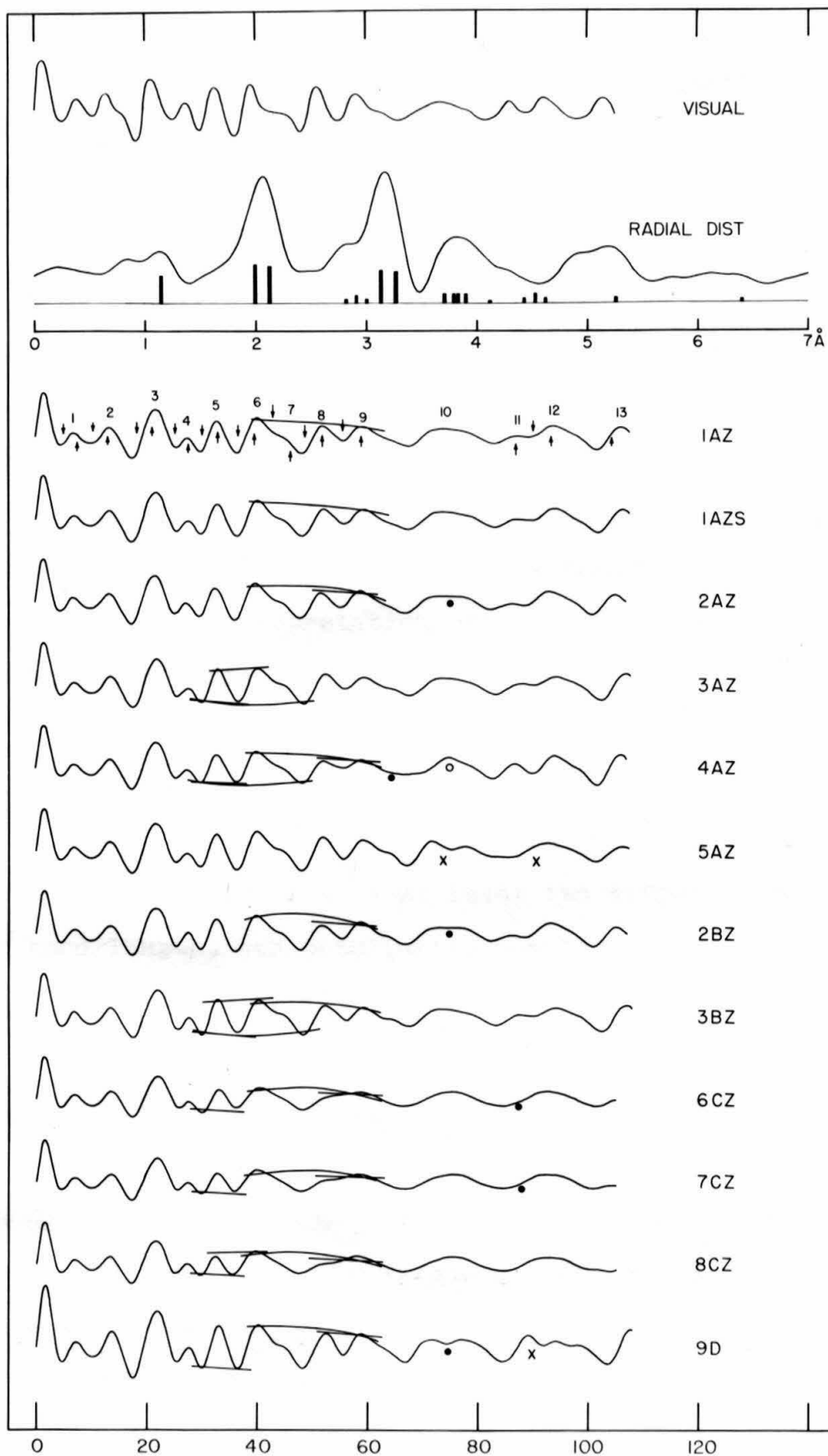


Figure 7. Molybdenum Hexacarbonyl

three and one-half. The possibility of a 2:2:2 MoC split has not been investigated in detail, but it is likely that a D_{2h} model with MoC distances of 1.97\AA , 2.05\AA , and 2.13\AA would not prove to be altogether unsatisfactory, even to the very limit of the known diffraction pattern. An increase in the relative temperature factor coefficients for adjacent CC, CO, and OO would improve the fit obtainable for the O_h models for values of q less than 65, but would not explain maximum 11, minimum 12, and maximum 12.

The determination of the scale factor for model 1 is presented in Table XVIII, and the final results are given in Table XIX. An interpretation of this structure is given in Section II of this thesis.

G. Osmium Tetroxide

The study of osmium tetroxide was undertaken to determine whether the existence of at least two different metal-ligand bond lengths was peculiar to hexaligated Mo, W, and U⁽²⁴⁾. A previous electron diffraction investigation⁽¹⁾ had led to a report of a regular tetrahedral molecule with OsO distance $1.66 \pm 0.05\text{\AA}$. Still another⁽²⁵⁾ had led to the conclusion that there exist two long and two short metal-ligand distances both in OsO_4 and RuO_4 ; however, these distances had the incredible values 1.79\AA and 2.81\AA for OsO_4 and 1.66\AA and 2.74\AA for RuO_4 . The symmetry D_{2h} was guessed from the observed lack of dipole moment⁽²⁶⁾.

TABLE XVIII

Scale Factor, Molybdenum Hexacarbonyl

Min	Max	q _{obs}	q _{calc} /q _{obs} (1A2)	Weights	
				I	II
1		5.0	0.991	0	0
	1	7.5	0.930	0	0
2		10.4	0.945	0	0
	2	13.0	1.032	0	0
3		18.2	0.957	0	0
	3	20.97	1.037	1	1
4		25.06	1.016	1	1
	4	27.28	1.006	1	2
5		29.86	0.998	1	1
	5	32.59	1.006	1	1
6		36.24	1.007	1	2
	6	39.1	1.023	1	0
7		42.5	-----	0	0
	7	45.6	-----	0	0
8		48.2	0.998	1	0
	8	51.43	1.009	1	2
9		55.08	1.010	1	3
	9	58.39	1.014	1	2
	11	86.0	1.014	1	0
12		89.1	1.003	1	0
	12	92.3	1.016	1	0
	13	103.1	1.028	1	0
AVERAGE I			1.012		
AVERAGE DEVIATION I			0.008		
AVERAGE II			1.011	SCALE FACTOR	
AVERAGE DEVIATION II			0.005		

TABLE XIX

Structure of Molybdenum Hexacarbonyl, C_{3v}

Parameter	Value	Limits of Error*
Mean CO	$1.14\overset{\circ}{\text{\AA}}$	$0.02\overset{\circ}{\text{\AA}}$
Short MoC	$1.99\overset{\circ}{\text{\AA}}$	$0.02\overset{\circ}{\text{\AA}}$
Split MoC	$0.13\overset{\circ}{\text{\AA}}$	$0.02\overset{\circ}{\text{\AA}}$
Long MoC	$2.12\overset{\circ}{\text{\AA}}$	$0.02\overset{\circ}{\text{\AA}}$
Split CO	$0.00\overset{\circ}{\text{\AA}}$	(assumed)
Angle CMoC	$90^\circ, 180^\circ$	(assumed)
Angle MoCO	180°	(assumed)

* Include $\pm 0.5\%$ estimated limit of scale error.

A sample of OsO_4 (Amend Drug and Chemical Company, New York City), generously provided by the Shell Development Company, was purified by vacuum sublimation and photographed with temperatures of the 40 cc sample bulb ranging from 60° to 70° . The electron wavelength was 0.06059\AA ; the camera distance, 10.94 cm.

The radial distribution curve of Figure 8 has peaks at 1.59\AA , 1.82\AA , and 2.81\AA , indicating without doubt an OsO split of about 0.23\AA and a generally tetrahedral arrangement of the oxygen atoms. The areas beneath the peaks, interpreted with the $Z_i Z_j$ approximation, indicate that the ratio of number of long OsO to number of short OsO is 1.5 and that the number of OO is 7.5 times as great as in the tetrahedral OsO_4 model, apparently partly because the $Z_i Z_j$ approximation is far from valid and partly because the fine details of the pattern were greatly over emphasized in the visual curve.

Table XX gives the parameter values assumed for the calculation of the curves of Figure 8; the OOsO angles have been assumed to be tetrahedral, as is consistent with the radial distribution curve. The values used for the relative temperature factor coefficients were calculated on the usual assumption of the simple valence potential function from the reported Raman spectrum⁽²⁷⁾ together with Badger's Rule⁽²²⁾. The values, of $a_{ij} \times 10^4$, were: short OsO , 0.0; long OsO , 0.4; and OO , 1.0. Account of the angle-variation in scattering power of O relative to Os was taken in all models.

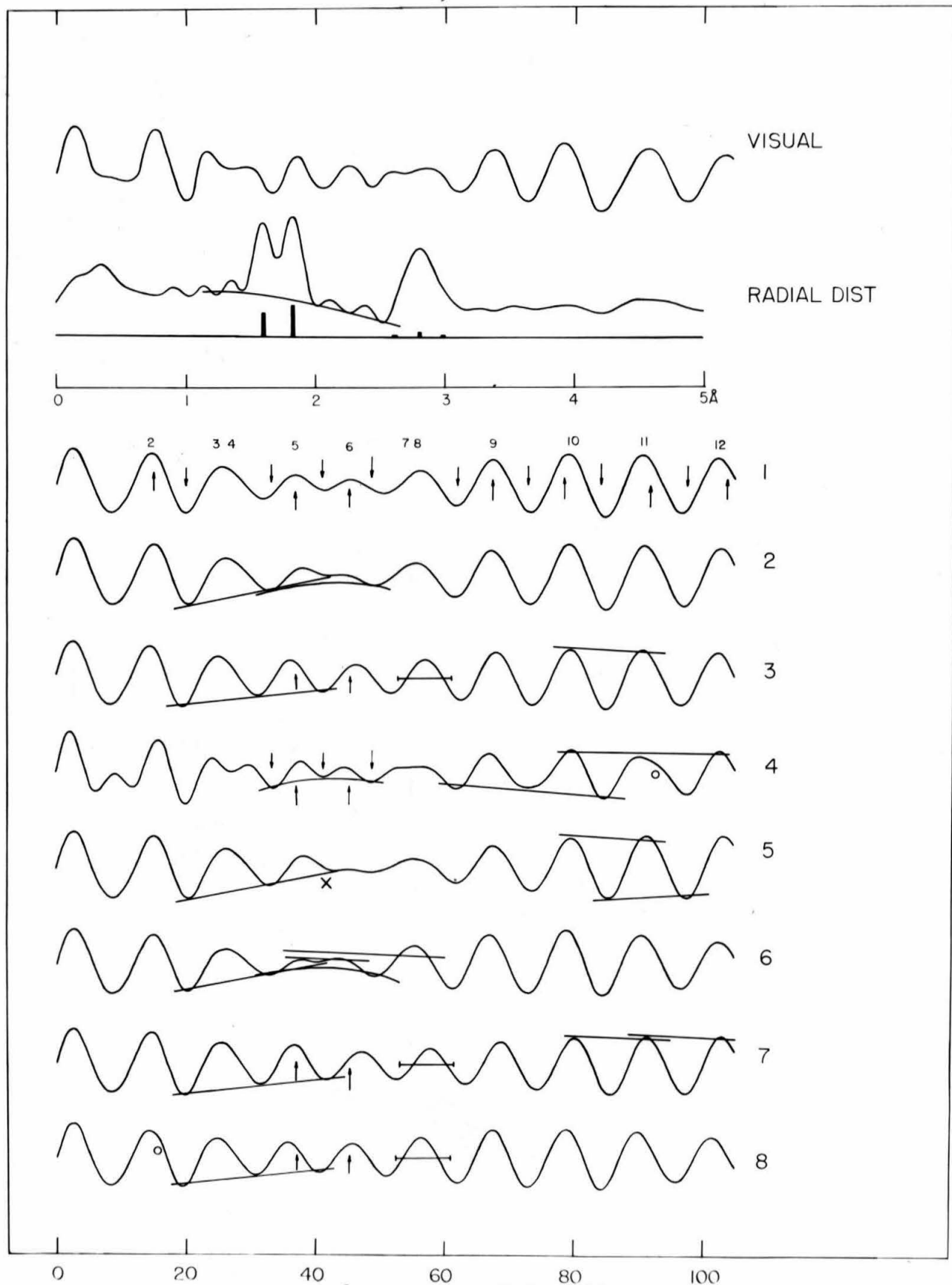


Figure 8. Osmium Tetroxide

TABLE XX

Values of Parameters, Osmium Tetroxide

Model	Symmetry	Long OsO	Short OsO	Scale Factor****
1*	**	1.82	1.59	1.004
2*	C _{2v}	1.82	1.59	1.005
3	C _{3v}	1.82	1.59	1.004
4*	C _{2v} ***	1.82	1.59	1.004
5	C _{2v}	1.80	1.59	1.016
6	C _{2v}	1.84	1.59	0.995
7	C _{3v}	1.80	1.59	1.014
8	C _{3v}	1.84	1.59	0.994

* Within the acceptable region of parameter space; unmarked models are unacceptable.

** Model 1 is 60% model 2 and 40% model 3.

*** Model 4 is model 2 with six times the theoretical weight for OO.

**** Determined according to weights II of Table XXI except for model 4, for which all features were given equal weight, but with the omission of 1 min, 1 max, and 2 min. Average deviation for model 4, 0.014.

The caricature of the intensity curve is fortunate for determining the general arrangement of the oxygen atoms but happens to be unfortunate for estimating the number of long and short OsO. For, minimum 7 of curve 2 is deepened either by increasing the OO weight, as in curve 4, or by increasing the number of long OsO, as in curve 3. On the other hand, if the measurements of maxima 5 and 6 are reliable — they may suffer from the St. John effect — curve 1 is better than curve 4. But in any event curve 4 is intolerable beyond q equals 70 besides being physically unjustifiable, so that curve 1, with the ratio 1.5 of number of long OsO to number of short OsO and otherwise clearly the most satisfactory, has to be judged the best.

Table XXI contains the determination of the scale factor; Table XXII, the structure. An interpretation of this structure is given in Section II of this thesis.

TABLE XXI

Scale Factor, Osmium Tetroxide

Min	Max	q _{obs}	q _{calc} /q _{obs} (1)	q _{calc} /q _{obs} (2)	q _{calc} /q _{obs} (3)	Weights	
						I	II
	1	7.7	-----	-----	-----	0	0
2		10.7	-----	-----	-----	0	0
	2	15.1	0.979	0.995	0.959	1	0
3		20.1	0.997	1.009	0.977	1	0
	3	23.2	-----	-----	-----	0	0
4		27.2	-----	-----	-----	0	0
	4	30.4	-----	-----	-----	0	0
5		33.3	0.961	0.988	0.936	1	0
	5	37.02	0.999	1.025	0.978	1	1
6		41.10	1.009	1.018	0.999	1	1
	6	45.26	1.010	0.989	1.026	1	1
7		48.6	1.042	1.017	1.064	1	0
	7	51.2	-----	-----	-----	0	0
8		53.8	-----	-----	-----	0	0
	8	58.4	-----	-----	-----	0	0
9		62.0	1.000	0.993	1.008	1	0
	9	67.52	1.000	0.996	1.008	1	1
10		72.71	1.009	1.006	1.014	1	1
	10	78.35	1.013	1.011	1.015	1	1
11		84.00	1.012	1.011	1.013	1	1
	11	91.71	0.990	0.992	0.990	1	1
12		97.39	0.994	0.996	0.991	1	1
	12	103.6	0.990	0.992	0.987	1	0
AVERAGE I			1.000	1.003	0.998		
AVERAGE DEVIATION I			0.012	0.011	0.022		
AVERAGE II			1.004	1.005	1.004	SCALE FACTOR	
AVERAGE DEVIATION II			0.007	0.010	0.013		

TABLE XXII

Structure of Osmium Tetroxide, $C_{2v} - C_{3v}$

Parameter	Value	Limit of Error*
Short OsO	1.596 ^o Å	0.03 ^o Å
Split OsO	0.231 ^o Å	0.02 ^o Å
Long OsO	1.827 ^o Å	0.02 ^o Å
Angles OOsO	109° 28'	(assumed)
Number long OsO	2.4	1.9 - 2.8
Number short OsO	1.6	1.2 - 2.1

* Including $\pm 0.9\%$ estimated limit of scale error.

References of Section I

1. L. O. Brockway, *Revs. Modern Phys.* 8, 231 (1936).
2. See for example, Ref. 6 and other recent publications on electron diffraction.
3. C. S. Lu and E. W. Malmberg, *Rev. Sci. Instruments*, 14, 271 (1943) (a equals 3.2492Å; c equals 5.20353Å).
4. R. Spurr and V. Schomaker, *J. Am. Chem. Soc.*, 64, 2693 (1942).
5. P. A. Shaffer, Jr., V. Schomaker, and L. Pauling, *J. Chem. Phys.*, 14, 659, 648 (1946).
6. M. Jones and V. Schomaker, *J. Chem. Phys.*, 19, 511 (1951).
7. See, for example, R. Trambarulo and W. Gordy, *J. Chem. Phys.*, 18, 1613 (1950); A. A. Westenberg, J. H. Goldstein, and E. B. Wilson, Jr., *J. Chem. Phys.*, 17, 1319 (1949); A. A. Westenberg and E. B. Wilson, Jr., *J. Am. Chem. Soc.*, 72, 199 (1950).
8. W. E. Anderson, R. Trambarulo, J. Sheridan, and W. Gordy, *Phys. Rev.*, 82, 58 (1951).
9. P. W. Allen and L. E. Sutton, *Acta Cryst.*, 3, 46 (1950).
10. J. N. Shoolery, R. G. Shulman, W. F. Sheehan, Jr., V. Schomaker, and D. M. Yost, *J. Chem. Phys.*, to be published.
11. A. L. Henne and M. Nager, *J. Am. Chem. Soc.*, 73, 1042 (1951).
12. A. L. Henne and W. G. Finnegan, *J. Am. Chem. Soc.*, 71, 298 (1949).
13. R. Trambarulo and W. Gordy, *J. Chem. Phys.*, 18, 1613 (1950).
14. V. Schomaker and D. P. Stevenson, *J. Am. Chem. Soc.*, 63, 37 (1941).
15. L. O. Brockway and H. O. Jenkins, *J. Am. Chem. Soc.*, 58, 2036 (1936).
16. N. W. Thibault, *Am. Mineral.*, 29, 249, 327 (1944); L. S. Ramsdell, *Am. Mineral.*, 29, 431 (1944), 30, 519 (1945).
17. L. O. Brockway and A. C. Bond, *Second Int. Cong. Cryst.*, Stockholm (1951), Abstr. ED12.
18. L. O. Brockway and N. R. Davidson, *J. Am. Chem. Soc.*, 63, 3287 (1941).

19. J. G. Aston, R. M. Kennedy, and G. H. Messerly, J. Am. Chem. Soc., 63, 2343 (1941).
20. L. O. Brockway, R. V. G. Ewens, and M. W. Lister, Trans. Faraday Soc., 34, 1350 (1938).
21. W. Rudorff and U. Hofmann, Z. physik. Chem., 28B, 351 (1935).
22. R. M. Badger, J. Chem. Phys., 2, 128 (1934), 3, 710 (1935).
23. W. Gordy, J. Chem. Phys., 14, 305 (1946).
24. S. H. Bauer, J. Chem. Phys., 18, 27 (1950).
25. H. Braune and K. W. Stute, Angew. Chem., 51, 528 (1938).
26. R. Linke, Z. physik. Chem., B48, 193 (1941). Private communication in 1938.
27. A. Langseth and B. Qviller, Z. physik. Chem., B27, 79 (1934).

II. MOLECULES WITH MULTIPLE VIBRATIONAL POTENTIAL MINIMA:

MoF_6 , WF_6 , UF_6 , $\text{Mo}(\text{CO})_6$, $\text{W}(\text{CO})_6$, OsO_4

A. The Equivalence of Non-equivalent Ligates

The diffraction experiments of Section I of this thesis indicate that in $\text{Mo}(\text{CO})_6$, $\text{W}(\text{CO})_6$, and OsO_4 there exist more than one metal-ligate bond distance. Recent diffraction experiments on $\text{UF}_6^{(1,2)}$, $\text{WF}_6^{(2)}$, and $\text{MoF}_6^{(2)}$ have confirmed the report⁽³⁾ that in these molecules the metal-fluorine distances are not all alike. For all these molecules, except possibly MoF_6 , this apparent lack of symmetry is quite certain, but for none of them is the evidence concerning the peripheral interatomic distances sufficient to define the over-all structure with certainty. On the other hand, the infrared and Raman spectra of $\text{UF}_6^{(4)}$; the Raman spectra of $\text{WF}_6^{(5)}$, $\text{MoF}_6^{(5)}$, and $\text{OsO}_4^{(6)}$; the agreement of observed and calculated entropies of $\text{UF}_6^{(7)}$; and the observation of a negligible or zero dipole moment in $\text{UF}_6^{(8)}$ and $\text{OsO}_4^{(9)}$ seem to indicate symmetrical structures.

These unsymmetrical structures have been chosen in as simple a fashion as possible to fit the results of the essentially instantaneous diffraction experiments; at any instant some of the metal-ligate distances must be different from the others. Being unsymmetrical, these structures seem to contradict the reasonable expectation of equivalence of these identical ligates. A realization of equivalence through a

coordinated interchange of roles among the ligates would increase the gross symmetry of each molecule. The consequences of this possibility for equivalence follow.

For the sake of simplicity, the structures of the hexafluorides will be considered in detail. All remarks about the hexafluorides may be extended readily by analogy to include the hexacarbonyls if fluorine atoms are replaced by carbonyl groups. The model which will be considered here is of C_{3v} symmetry with all fluorine-metal-fluorine angles approximately right angles. If, then, resonance is allowed such that movement of fluorine A to a position close to the central atom must be accompanied by the movement outwards of fluorine B directly across from A, and such that movement of A outwards necessitates the movement of B inwards, the symmetry C_{3v} is preserved at all times. The problem is then to determine whether the equivalence so attained, in which a pair of opposed fluorine atoms tunnels through the potential barrier which separates their equilibrium positions relative to the remainder of the molecule, explains the apparent contradiction of experimental facts, one set affirming cubic symmetry and the other set denying cubic symmetry.

The ground states of these hexafluorides and hexacarbonyls are each eight-foldly degenerate, corresponding to the ratio of the orders of the rotational subgroups of O_h and C_{3v} . Or, geometrically, this eight-fold degeneracy corresponds to the eight equivalent positions, at the corners of a cube, of the central atom relative to the center of mass of its ligates.

It is convenient to let all the adjacent fluorine-metal-fluorine angles be exactly right angles and to choose three independent coordinates to describe the eight-fold minimum problem. Each of these coordinates is taken as the distance along the line joining them that a pair of opposite fluorine atoms moves with respect to the remainder of the molecule. Of course, in the actual molecule there will most probably be interaction among these doubling vibrations and interaction of them with all the other vibrations of the molecule. However, a continuous transition from the actual state to the ideal state of independent coordinates can be made since the interaction may be imagined to be as small as desired without changing the essence of the situation.

Such an apparently continuous transition cannot always be made. It is a well known fact⁽¹⁰⁾ that in the calculation of the partition function of ammonia the summation over the low-lying vibrational levels may be made equally well by using the symmetry number six and counting every level or by using the symmetry number three and counting every doubled level as one level. If the attempt were made continuously to deform the non-planar equilibrium configuration of ammonia into a planar equilibrium configuration under the constraint of maintaining unchanged all energy levels by appropriate variations in the form of the potential energy, then as the molecule at last became exactly planar its partition function

would be calculated by summing over each component of the doubled levels and using the symmetry number six. However, the correct way to calculate the partition function of a real planar ammonia molecule is to use the symmetry number six and to count actually occurring^{sc} levels, which in this case would be single and equal in number to the number of doubled levels in the continuously deformed molecule. The continuous variation to planarity with preservation of energy levels demands the rise of an infinitely high potential barrier between equivalent potential minima, and thus at planarity there would exist two forms of ammonia molecules with planar equilibrium configuration. Between these two forms transitions would be strictly forbidden; one form would occupy one-half the doubled levels and the other form the other half. This attempted continuous variation is accordingly really discontinuous if only one form of planar molecule is to exist.

In Figure 1 are given the species and quantum numbers of the vibrational energy levels of the three independent and equivalent doubling coordinates. Their independence and equivalence causes each to have the same vibrational frequency and also leads naturally to their description in terms of an F_{1u} -like vibration for symmetry O_h . Although this vibration is only an idealization, the doubling coordinates involving only stretching, the real vibration analogous to it is primarily stretching and is quite similar to it. On the other hand, if Figure 1 is considered to be a description of a model with C_{3v} pseudosymmetry, then the frequencies of the

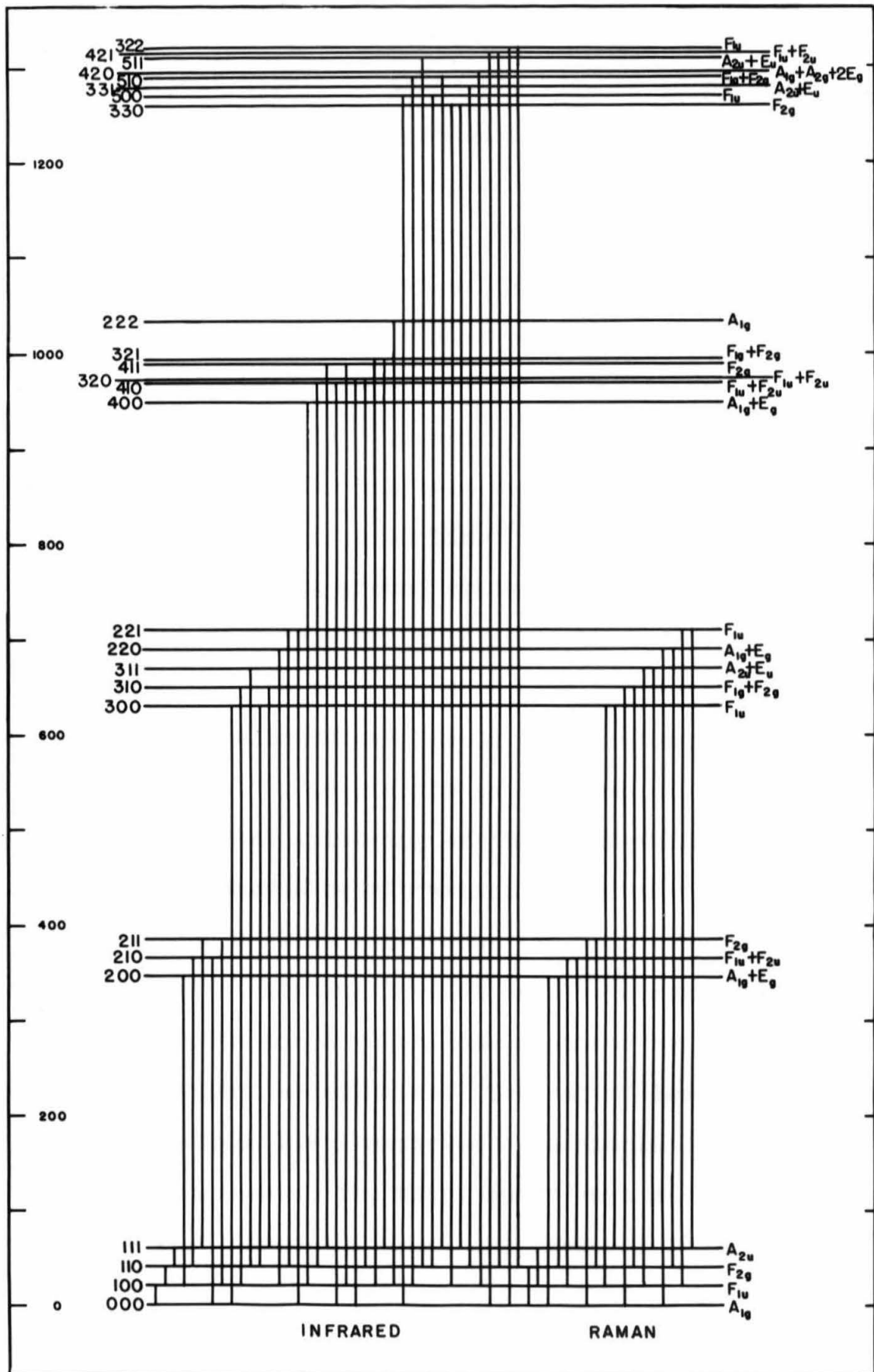


Figure 1. Uranium Hexafluoride

A_1 and E vibrations most perturbed by the existence of the eight equivalent C_{3v} -like minima are assumed to be equal, this equality of frequencies being accomplished through a suitable choice of force constants in the vibrational potential energy for each C_{3v} -like minimum.

The quantum numbers of Figure 1 are even and odd for symmetric and antisymmetric states of each of the independent doubling coordinates. The energy of the split in the ground vibrational state of UF_6 , for which the energy scale of Figure 1 has been drawn, has been evaluated from an assignment of the 675 cm^{-1} infrared line⁽⁴⁾ to transitions from the eight-foldly degenerate ground state to the eight-foldly degenerate set of levels which in a simple O_h model would correspond to the 656 cm^{-1} A_{1g} Raman-active frequency. In general, all the vibrational levels of a molecule such as this are eight-foldly degenerate as referred to O_h symmetry. The magnitude of the splitting of the eight-fold degeneracy increases with increasing vibrational quantum number only very slowly for those O_h -like vibrations (in this case, bendings and symmetrical stretchings) which involve during their course very little of the ideal vibration described by the triply degenerate doubling coordinates. The set of levels which replaces the single level expected of a simple O_h molecule for its A_{1g} fundamental is, then, split just as the ground state is split. Since the usual symmetry selection rules for O_h apply for transitions between the individual levels, infrared transitions to this set of A_{1g} -like levels occur displaced

from the main Raman frequency by the split of the ground state from A_{1g} to F_{1u} . The main Raman line is assumed to be given by the transitions from the ground state levels to the excited state levels which involve no change in the quantum numbers of Figure 1.

The infrared and Raman transitions which are allowed by the symmetry selection rules for O_h are very numerous, as indicated in Figure 1. However, the intensities of lines which involve the change of two quantum numbers at once are reasonably expected to be small. If such lines are forbidden, the circumstance that groups of transitions in Figure 1 involve equal energies serves to bring the potentially complicated situation into fair agreement with the simplicity of the observed spectra^(4,5). Accordingly, the infrared spectrum of Figure 1 then has only five different lines, at 20 cm^{-1} , 330 cm^{-1} , 630 cm^{-1} , 930 cm^{-1} , and 1290 cm^{-1} ; and the Raman spectrum of Figure 1 then has only two different lines, at 350 cm^{-1} and 610 cm^{-1} . An estimate of the magnitude of the dipole moment and polarizability matrices for these seven lines indicates that the infrared lines are expected to be intense and the Raman lines, weak even as Raman lines. The infrared line at 630 cm^{-1} in Figure 1 corresponds to the observed⁽⁴⁾ intense absorption at about 623 cm^{-1} in UF_6 .

The effect of degeneracy upon excited levels is conveniently predicted with the use of the triply degenerate doubling coordinates which are each formally like the coordinates

ordinarily chosen to describe the inversion doubling in ammonia. The double minimum problem has been investigated theoretically several times⁽¹¹⁾. The exact theoretical solution⁽¹²⁾ for a potential of the form

$$V(x) = \left(\frac{x^6}{12x_0^4} - \frac{x^2}{4} + \frac{x_0^2}{6} \right) \frac{h\nu}{2}$$

does not seem inappropriate here. This potential will ensure that the fluorine atoms remain at a reasonable distance from the central atom, and since only the very low-lying vibrational levels are of interest here the exact way in which the potential rises to very large values for large values of x is probably unimportant. The parameter x_0 depends on the distance $2q_0$ between minima, on the frequency ν of the unperturbed vibration, and on the reduced mass μ thus:

$$x_0 = 2\pi q_0 \sqrt{\frac{\mu\nu}{h}}$$

Values of the symmetric and antisymmetric energy levels of the vibration as functions of x_0 are given in the original article⁽¹²⁾ and have been recalculated. In Table I are given values of x_0 appropriate to ammonia, the hexafluorides, and the hexacarbonyls. The values of $2q_0$ used were the observed splits in distances rather than the distances between minima of potentials which would match the various observed densities of scattering matter, since the additional separation of the maxima through contributions from excited vibrational states is not readily estimated.

TABLE I

Order of Magnitude of Splitting of Ground States

Molecule	x_0	Predicted Values		Observed Values
		Height of Potential Barrier (cm^{-1})	Split of Ground State (cm^{-1})	Split of Ground State (cm^{-1})
NH_3	3.2	800*	20	0.7
UF_6	3.3	440	10	19.0
UF_6	3.8	810	small	19.0
WF_6	3.2	640	15	----
MoF_6	2.0	240	220	----
$\text{W}(\text{CO})_6$	2.7	250	30	----
$\text{Mo}(\text{CO})_6$	1.5	80	210	----

* Best value is $2076 \text{ cm}^{-1}(13)$.

The value of ν , the higher frequency of species F_{lu} in a simple O_h model, was taken to be the same as the symmetrical stretching frequency; this frequency has been observed in the Raman spectra^(4,5) for the hexafluorides and was estimated from Badger's Rule⁽¹⁴⁾ for the hexacarbonyls. The frequency used for UF_6 in the case for which x_0 is 3.3 is 480 cm^{-1} and was obtained by the use of the three observed Raman frequencies⁽⁴⁾ and of the valence bond potential of Wilson described for use in calculations of SF_6 , SeF_6 , and TeF_6 ⁽¹⁵⁾. In all cases the reduced mass $\frac{2m(M + 4m)}{M + 6m}$ was used, where M is the mass of the metal atom and m is the mass of the ligate, CO being considered a unit. Table I contains values of the splits in the ground states and the heights of the various potential barriers calculated from the values of x_0 . The values are intended to indicate only the order of magnitude to be expected.

Wave functions for the symmetric and antisymmetric levels of the ground vibrational state of this sort of system were calculated for x_0 equals 3.00. Evaluation of the density of scattering matter from these wave functions shows that there are indeed two maxima in scattering matter and that the density midway between the maxima is about one-tenth of the value of one of the maxima. Since the distance between maxima in scattering matter is less than the distance between minima of the potential function, the values of x_0 are all somewhat small, especially those for MoF_6 and $Mo(CO)_6$. Moreover, calculations have not been made to determine whether the density

of scattering matter for values of x_0 near 1.5 has two maxima to correspond to the diffraction data.

The energies of 200, 210, and 211 for UF_6 as shown in Figure 1 are the result of the identification of the 623 cm^{-1} absorption and the estimated split of the fundamental with the use of the predicted F_{1u} frequency, 480 cm^{-1} . This value is probably too small by about 15% since the predictions for the F_{1u} vibrations of SeF_6 and TeF_6 with a similar use of Wilson's⁽¹⁵⁾ potential are too small relative to the observed values⁽¹⁶⁾ by about 15%. If 480 cm^{-1} is indeed too small, the value of x_0 should be increased, and the group 200, 210, 211 should lie closer to the group 300, 310, 311.

The value of the higher F_{1u} frequency, if corrected by 15%, is about 570 cm^{-1} instead of 480 cm^{-1} ; 570 cm^{-1} is somewhat less than the value 640 cm^{-1} which has been assigned⁽⁴⁾. This discrepancy, together with the fact that a split of 19 cm^{-1} in the ground state is not unreasonable, strengthens somewhat the new assignments of the infrared lines at 675 cm^{-1} and 623 cm^{-1} , especially since the original assignment⁽⁴⁾ depends on the existence of an accidental degeneracy at 640 cm^{-1} and full use of the three parameters: two infrared-active frequencies and an inactive frequency. However, any meaningful reinterpretation of this spectrum in terms of the model proposed here would require not only a careful consideration of weak lines, as yet unobserved, but also a knowledge of the spectrum beyond 17 microns.

The explanation of the simplicity of the Raman spectra of these hexafluorides^(4,5) depends on the selection rule which forbids changes in two quantum numbers at once, the absence of an increase in split with vibrational quantum number in the Raman-like vibrations, and the estimation that the polarizability matrix for allowed transitions like those of Figure 1 is small. It is possible that weak lines are still to be observed in the Raman spectra. The infrared and Raman spectra of the hexacarbonyls have not been reported.

Formal calculation of the split in the degeneracy of the ground state of XY_6 ($C_{3v} - O_h$) is of interest. The wave functions, Ψ_i , describe the states of the system in terms of the approximately normalized, but non-orthogonal, electronic wave functions, u_i , for each of the non-interacting C_{3v} -like structures:

$$\begin{aligned}\Psi_a(A_{1g}) &= N_a(u_1 + u_2 + u_3 + u_4 + u_5 + u_6 + u_7 + u_8) \\ \Psi_b(F_{1u}) &= N_b(u_1 + u_2 - u_3 - u_4 + u_5 + u_6 - u_7 - u_8) \\ \Psi_c(F_{1u}) &= N_c(u_1 - u_2 - u_3 + u_4 + u_5 - u_6 - u_7 + u_8) \\ \Psi_d(F_{1u}) &= N_d(u_1 + u_2 + u_3 + u_4 - u_5 - u_6 - u_7 - u_8) \\ \Psi_e(F_{2g}) &= N_e(u_1 - u_2 + u_3 - u_4 + u_5 - u_6 + u_7 - u_8) \\ \Psi_f(F_{2g}) &= N_f(u_1 + u_2 - u_3 - u_4 - u_5 - u_6 + u_7 + u_8) \\ \Psi_g(F_{2g}) &= N_g(u_1 - u_2 - u_3 + u_4 - u_5 + u_6 + u_7 - u_8) \\ \Psi_h(A_{2u}) &= N_h(u_1 - u_2 + u_3 - u_4 - u_5 + u_6 - u_7 + u_8).\end{aligned}$$

The energy levels obtained from these by perturbation theory are:

$$W(A_{1g}) = W^0 + \frac{(1H'1) + 3(1H'2) + 3(1H'3) + (1H'7)}{1 + 3(1,2) + 3(1,3) + (1,7)}$$

$$W(F_{1u}) = W^0 + \frac{(1H'1) + (1H'2) - (1H'3) - (1H'7)}{1 + (1,2) - (1,3) - (1,7)}$$

$$W(F_{2g}) = W^0 + \frac{(1H'1) - (1H'2) - (1H'3) + (1H'7)}{1 - (1,2) - (1,3) + (1,7)}$$

$$W(A_{2u}) = W^0 + \frac{(1H'1) - 3(1H'2) + 3(1H'3) - (1H'7)}{1 - 3(1,2) + 3(1,3) - (1,7)}$$

If (1,2), (1,3), (1,7), (1H'3), and (1H'7) are zero, this set of energy levels is equivalent to those of Figure 1.

An estimate of the order of magnitude of the splitting of the ground state of UF_6 can be made independently of the spectrum. The observed entropy has been calculated from data on the heat capacity observed above $14^\circ K$ ⁽¹⁷⁾. The entropy for the $C_{3v} - O_h$ model is greater than that for the O_h model by about $R \log 8$, and a rise in the heat capacity below about 14° is expected, corresponding to residual entropy of about $R \log 8$. The difference in energy of the ground state and the seven other low-lying levels is of the order of kT at $14^\circ K$, or about 10 cm^{-1} . This estimate, of course, assumes that the heat capacity measurements were made at equilibrium and that this residual entropy is not lost at a higher temperature by interactions among the molecules in the crystal.

From measurements of the dielectric constant of UF_6 , the molar polarization has been found to be $30.7 \pm 1.0 \text{ cc}$ at 19.6° ⁽¹⁸⁾ and $27.1 \pm 0.3 \text{ cc}$ at 59.5° , 67.4° , and 89.0° ⁽⁸⁾. The work of

these two groups of observers seems to be equally reliable, but is certainly contradictory. If a mean temperature of 72° is used with the value 27.1 cc together with the value of 30.7 cc at 19.6° , a dipole moment of 1.1 ± 0.3 Debye is found for UF_6 . Since the molar refraction (Na D) is only 21.83 cc⁽⁸⁾, a dipole moment of 0.55 Debye is not impossible even if the value of the molar polarization at 19.6° is disregarded.

Although a simple O_h model readily explains a zero dipole moment, it does not satisfactorily account for the need to discount the measurements at 19.6° or for the anomalously large molecular polarization which is required by a zero dipole moment. If, however, it is admitted that the C_{3v} -like model proposed may accidentally have a dipole moment which is as small as 1.1 Debye, then all except the reported temperature-independence of the dielectric constant from 60° to 90° is explained satisfactorily.

Detailed interpretation of the structure of OsO_4 is complicated by the observation in Section I G. of this thesis that neither a 2:2 nor a 3:1 split in OsO distances is alone satisfactory. Consequently, a simple assumption about symmetry which will serve as a good approximation throughout is not at hand. It is clear, nevertheless, that if the pseudosymmetry is C_{2v} , that the ground state is six-foldly degenerate with vibrational states of species A_1 , F_2 , and E ; and if the pseudosymmetry is C_{3v} , the ground state is four-foldly degenerate with vibrational states of species A_1 and F_2 . A quantum

mechanical calculation, as for XY_6 , of the energies of these degenerate states of the $C_{2v} - T_d$ model with the use of the wave functions

$$\begin{aligned}\Psi_a(A_1) &= N_a(u_1 + u_2 + u_3 + u_4 + u_5 + u_6) \\ \Psi_b(F_2) &= N_b(u_1 - u_6) \\ \Psi_c(F_2) &= N_c(u_2 - u_4) \\ \Psi_d(F_2) &= N_d(u_3 - u_5) \\ \Psi_e(E) &= N_e(u_1 + u_6 - \frac{1}{2}(u_2 + u_3 + u_4 + u_5)) \\ \Psi_f(E) &= N_f(u_2 - u_3 + u_4 - u_5)\end{aligned}$$

leads to the energies

$$\begin{aligned}W(A_1) &= W^0 + \frac{(1H'1) + 4(1H'2) + (1H'6)}{1 + 4(1,2) + (1,6)} \\ W(F_2) &= W^0 + \frac{(1H'1) - (1H'6)}{1 - (1,6)} \\ W(E) &= W^0 + \frac{(1H'1) - 2(1H'2) + (1H'6)}{1 - 2(1,2) + (1,6)}.\end{aligned}$$

Similarly, for a $C_{3v} - T_d$ model, the wave functions and energy values are:

$$\begin{aligned}\Psi_a(A_1) &= N_a(u_1 + u_2 + u_3 + u_4) \\ \Psi_b(F_2) &= N_b(u_1 + u_2 - u_3 - u_4) \\ \Psi_c(F_2) &= N_c(u_1 - u_2 + u_3 - u_4) \\ \Psi_d(F_2) &= N_d(u_1 - u_2 - u_3 + u_4) \\ W(A_1) &= W^0 + \frac{(1H'1) + 3(1H'2)}{1 + 3(1,2)} \\ W(F_2) &= W^0 + \frac{(1H'1) - (1H'2)}{1 - (1,2)}.\end{aligned}$$

The lack of a dipole moment in OsO_4 seems to be certain, since the temperature was varied over a great range⁽⁹⁾. If neither the dipole moment data nor the diffraction data are to be denied, then the dipole moment must be negligible by accident. The simplicity of the Raman spectrum⁽⁶⁾, even though lines may have escaped observation, demands explanation, perhaps of the same sort as was given for UF_6 .

The standard entropy of $\text{OsO}_4(\text{g})$ has been calculated⁽¹⁹⁾ with the assumption of simple T_d symmetry; an experimental value is not available. Presumably the low temperature heat capacity shows that the solid has residual entropy, which may vanish at attainable temperatures because the possibility of interactions among molecules in the crystal is greater for OsO_4 than for a sexiligated compound.

B. The Nature of the Non-equivalent Bonds

Of immediate interest after a recognition of the real equivalence of each ligate is the reason why non-equivalent bonds should have existence at all, when it is possible for the central atom to form strong and equivalent bonds in a much simpler and more conventional fashion. The fact that sexiligated and quadriligated metal atoms exhibit these non-equivalent bonds to equivalent ligates indicates that the formation of these bonds is not an accident of a particular kind of hybridization of atomic orbitals; the fact that hexafluorides and hexacarbonyls exhibit this sort of bonding indicates that their formation is not an accident of the

availability of certain bonding orbitals or an accident of ionic character, unless the carbon in each carbonyl group be considered a conductor of electrons from metal to oxygen.

The abundance of stable d orbitals and the absence of relatively stable p orbitals for use in sigma-bonds together with the availability of the excess of stable orbitals for use in pi bonds distinguish the bonding situation in MoF_6 and WF_6 from that in TeF_6 , a molecule of simple O_h symmetry. For Te has d orbitals available which are somewhat less stable than its s and p orbitals; as a result, use of the d orbitals is minimized. On the other hand, use of more than two of the stable d orbitals of W and Mo in sigma-bonds necessitates abandonment of O_h symmetry for the sigma-bonds. Presumably, the extra d-character of the sigma-bonds and the formation of pi-bonds with the excess of stable orbitals would lower the energy of the molecule. These pi-bonds would be formed in the hexafluorides by a transfer of electrons from the fluorine atoms to the metal atom in order to relieve the positive charge on the metal atom caused by ionic character in the six sigma-bonds. In the carbonyls these pi-bonds would be formed by the three unshared pairs of electrons on the metal atom in an effort to decentralize the large negative charge caused by the carbonyls' contributing all the bonding electrons of the sigma-bonds. And ionic character of the bonds through carbon not only would contribute to the exodus of the metallic electrons but also would allow the use of d orbitals in bonding rather than the less stable p orbitals,

extra d-character seeming also to contribute bond strength beyond that predicted by the usual Pauling strength criterion. In view of the previous successes in predicting symmetry from the symmetry of the sigma-bond hybridization, as in symmetrical molecules like CO_2 which have resonating multiple bonds, hybridization to form non-equivalent sigma-bonds, as already suggested for $\text{UF}_6^{(20)}$, seems to be the reason for asymmetry.

Eight stable orbitals are available on Os for the formation of tetrahedral double bonds, the average OsO distance indicating that this is a good approximation to the structure. But whether or not these double bonds can be made equivalent is not known; however, the most stable set may well require a decrease in symmetry. The unused, stable 6p and 5d orbitals and the unstable 6d orbitals on Os are available for use in triple bonds.

How to interpret these non-equivalent bonds quantitatively in terms of Pauling's⁽²¹⁾ use of extra d-character and varying bond orders has not been investigated. Since the d-character of the sigma bonds is unknown, $\text{Mo}(\text{CO})_6$ being diamagnetic⁽²²⁾ and the hexafluorides showing only feeble temperature-independent paramagnetism⁽²³⁾, and since the very definition of d-character of bonds which have d orbitals used for pi-bond formation is lacking, such an interpretation must be ambiguous because the domains of d-character and bond order are coextensive: the lengths of bonds. It is perhaps sufficient, then, to note that the average metal-ligand distance corresponds to a single bond in the sexilicates and to a double bond in OsO_4 , lengths to be expected according to simple valence theory.

References of Section II.

1. S. H. Bauer, J. Chem. Phys., 18, 27 (1950).
2. O. Bastiansen, unpublished.
3. H. Braune and P. Pinnow, Z. physik. Chem., B35, 239 (1937).
4. J. Bigeleisen, M. G. Mayer, P. C. Stevenson, and J. Turkevich, J. Chem. Phys., 16, 442 (1948).
5. K. N. Tanner and A. B. F. Duncan, J. Am. Chem. Soc., 73, 1164 (1951).
6. A. Langseth and B. Qviller, Z. physik. Chem., B27, 79 (1934).
7. S. H. Bauer, J. Chem. Phys., 18, 994 (1950).
8. C. P. Smyth and N. B. Hannay, Princeton Report A2130, Oct. 1, 1944.
9. R. Linke, Z. physik. Chem., B48, 193 (1941).
10. K. S. Pitzer, J. Chem. Phys., 7, 251 (1939).
11. See reference (10) and its references.
12. P. M. Morse and E. C. G. Stückelberg, Helv. Phys. Acta, 4, 337 (1931).
13. M. F. Manning, J. Chem. Phys., 3, 136 (1935).
14. R. M. Badger, J. Chem. Phys., 2, 128 (1934); 3, 710 (1935).
15. D. M. Yost, C. C. Steffens, and S. T. Gross, J. Chem. Phys., 2, 311 (1934).
16. H. Sachsse and E. Bartholome, Z. physik. Chem., B28, 257 (1935).
17. See references (1) and (7) for references.
18. C. B. Amphlett, L. W. Mullinger, and L. F. Thomas, Trans. Faraday Soc., 44, 927 (1948).
19. L. H. Anderson and D. M. Yost, J. Am. Chem. Soc., 60, 1822 (1938).
20. F. G. Fumi and G. W. Castellan, J. Chem. Phys., 18, 762 (1950).
21. L. Pauling, Proc. Roy. Soc., A196, 343 (1949).
22. P. Ray and H. Bhar, J. Indian Chem. Soc., 5, 497 (1928).
23. W. Tilk and W. Klemm, Z. anorg. allgem. Chem., 240, 355 (1939).

III. THE DISSOCIATION ENERGIES OF DIATOMIC MOLECULES AND THE ENERGIES OF THE VALENCE STATES OF ATOMS

A. The Dissociation Energy of Carbon Monoxide and the Heat of Sublimation of Graphite

Reprinted from the Proceedings of the NATIONAL ACADEMY OF SCIENCES,
Vol. 35, No. 7, pp. 359-363. July, 1949

THE DISSOCIATION ENERGY OF CARBON MONOXIDE AND THE HEAT OF SUBLIMATION OF GRAPHITE

BY LINUS PAULING AND WILLIAM F. SHEEHAN, JR.

GATES AND CRELLIN LABORATORIES OF CHEMISTRY, CALIFORNIA INSTITUTE OF
TECHNOLOGY*

Communicated May 5, 1949

For a number of years there has existed doubt about the value of the dissociation energy of carbon monoxide and about the heat of sublimation of graphite, a directly related quantity. The most popular values for the dissociation energy of carbon monoxide are 9.144 electron-volts, suggested by Herzberg¹ on the basis of predissociation phenomena in band spectra, 9.61 e. v., suggested by Hagstrum and Tate² on the basis of electron impact experiments (or the value 9.85 e. v. derivable from predissociation data³), and 11.11 e. v., suggested by Gaydon and Penney⁴ from an analysis of spectroscopic data. These values together with thermochemical data lead to the values 124.9, 141.4, and 170.3 kcal./mole, respectively, for the heat of sublimation of graphite. Strong evidence for the last of these values has been presented by Brewer, Gilles, and Jenkins,⁴ who have reported 170.4 kcal./mole from a direct experimental determination. The value has, however, been criticized by other investigators,^{6, 7} and has been defended by Brewer.⁸

In this paper we communicate an argument which indicates that the high values of about 170 kcal./mole for the heat of sublimation of carbon to $C_{(g)}(^3P)$ and 11.11 e. v. for the dissociation energy of carbon monoxide are not correct, and which leads instead to the values 140 kcal./mole and 9.77 e. v., respectively.

The argument is based on the postulate that the linear extrapolation of the vibrational levels for the lower vibrational states of a molecule (a linear Birge-Sponer extrapolation) leads to an energy value corresponding to the dissociated atoms in a hypothetical electronic state called the valence state. An atom in the valence state, as defined in this paper, is an isolated atom with the same electronic structure as that which the atom has in the molecule under consideration. It is the state that would result if the atoms in the molecule were to be pulled apart without change in the electronic structures that exist in the molecule in the lower vibrational levels of the lower electronic state. The wave function for the valence state of an atom may of course be formed by linear combination of those for its spectroscopic states, and the energy of the valence state is somewhat higher than that of the normal spectroscopic state, by an amount, the valence-state energy, that is reasonably constant for a given atom from molecule to molecule.^{9, 10}

The valence-state energy of the oxygen atom has been evaluated as 0.74 ± 0.05 e. v.¹⁰ A rough value for the valence-state energy of nitrogen can be calculated from spectroscopic data for the three low-energy levels of the atom, all based on the configuration $2s^22p^3$. These levels, 4S , 2D , and 2P , have energy values F° , $F^\circ - 6/25 F^2$, and $F^\circ - 15/25 F^2$, respectively, according to simple spectroscopic theory. The states 2D and 2P are observed to lie at energies 2.38 e. v. and 3.57 e. v. above the normal state 4S . These values are not in the ratio 3:5 given by the simple theory, and accordingly there is uncertainty as to the value of the resonance integral F^2 . The normal valence state of nitrogen to the extent that it is based on the normal configuration $2s^22p^3$ is the state in which each of three electrons occupying separate p orbitals has its spin oriented independently of the other two electrons, the corresponding energy being $F^\circ - 21/50 F^2$. Because of the uncertainty in the value of F^2 , the energy of the valence state cannot be predicted precisely. If the 4S level is considered to be depressed by resonance with a similar state based on an excited configuration of the atom the valence-state energy would be calculated to be 1.39 e. v., whereas if the 2P level is considered to be depressed by resonance the valence-state energy would be 1.19 e. v. A value somewhat larger than either of these values might be expected to result from contributions of higher spectroscopic states to the valence state.

A more reliable value for the valence-state energy of the nitrogen atom can be obtained from the consideration of nitric oxide. The energy of

dissociation of the normal nitric oxide molecule to a nitrogen atom and an oxygen atom in their valence states is found by linear extrapolation of the low-lying vibrational levels to be 7.87 e. v. If we subtract from this quantity the sum of the valence-state energy of oxygen, 0.74 e. v., and that of nitrogen, approximately 1.5 e. v., the dissociation energy D_0 is predicted to be approximately 5.6 e. v. This argument hence favors the value $D_0 = 5.29$ e. v. proposed by Mulliken¹¹ and supported by Wulf¹² and Hagstrum,¹³ rather than the value 6.49 e. v. supported by Gaydon.¹⁴ If we accept the value 5.29, the valence-state energy of the nitrogen atom is calculated to be 1.84 e. v.

Some substantiation of this value is provided by the consideration of the normal state and the first excited state of the nitrogen molecule. The energy of dissociation of N_2 in its normal state $X^1\Sigma_g^+$ into two nitrogen atoms in their valence states is found by linear extrapolation to be 11.60 e. v., and the value of this quantity given by the first excited state $A^3\Sigma_u^+$ is 10.58 e. v. On subtracting the dissociation energy of the nitrogen molecule, 7.38 e. v. (the alternative spectroscopic value 9.76 e. v. is to be eliminated as not leading to sufficiently large values for the valence-state energy and being incompatible with the results of electron-impact experiments¹³), and dividing by 2, we obtain 2.11 and 1.60 e. v., respectively, for the valence-state energy of the nitrogen atom. The value 2.11 e. v. given by the normal state of the nitrogen molecule is probably high because of a large amount of s character in the orbital of the σ bond for this molecule. We conclude that the normal valence-state energy of the nitrogen atom is approximately 1.84 e. v., and that variation of a few tenths of an electron-volt may be expected.

The valence-state energy of the carbon atom can be similarly derived from spectroscopic data for the molecules CH and C_2 . For the normal state of CH the energy of dissociation to a carbon atom and a hydrogen atom in their valence states is 5.20 e. v., as given by linear extrapolation, and the dissociation energy D_0 to the atoms in their normal states is 3.47 e. v. The difference, 1.73 e. v., can be taken as the valence-state energy of the carbon atom, inasmuch as the valence state and the normal spectroscopic state of the hydrogen atom are essentially the same. For the normal C_2 molecule the energy of dissociation to two carbon atoms in their valence states is found by linear extrapolation to be 7.05 e. v., and the dissociation energy D_0 is 3.6 e. v. These quantities lead to 1.73 e. v. for the valence-state energy of carbon, in exact agreement with the preceding value.

The energy of a carbon atom in its valence state and an oxygen atom in its valence state relative to the normal state of the carbon monoxide molecule is found to be 11.23 e. v. by linear extrapolation for the normal state, and the values 12.33, 11.87, and 12.10 e. v. are similarly obtained for

the first three excited states of the molecule, $a\ ^3\Pi$, $a'\ ^3\Sigma$, and $A\ ^1\Pi$. If we subtract from these numbers the quantity 2.47 e. v., the sum of the valence-state energies for carbon and oxygen, as evaluated above, we obtain 8.76, 9.86, 9.40 and 9.63 e. v. for the dissociation energy of the normal carbon monoxide molecule to atoms in their normal spectroscopic states. These values are incompatible with the high value 11.11 e. v. for $D_0(\text{CO})$, and may be considered to support either the value 9.14 or the value 9.61–9.85.

Evidence indicating that the second of these values, 9.6–9.85, is correct is obtained from the discussion of the cyanogen molecule and the cyanide radical. Linear extrapolation of the vibrational levels of the lowest state of the CN molecule, $X\ ^2\Sigma^+$, leads to 9.85 e. v. for the energy of a carbon atom and a nitrogen atom in their valence states relative to the normal state of the molecule. On subtracting 1.73 for the valence-state energy of carbon and 1.84 for that of nitrogen, we obtain 6.28 e. v. for $D_0(\text{CN})$. This value strongly supports the spectroscopic value 6.24 e. v. for this molecule,¹⁴ rather than the alternative spectroscopic value 7.50 e. v. From thermochemical data and the accepted dissociation energy of the oxygen molecule, 5.08 e. v., it can be calculated¹⁵ that the dissociation energy of cyanogen, C_2N_2 , into two CN molecules is given by the equation

$$D_0(\text{NC-CN}) = 2D_0(\text{CO}) + D_0(\text{N}_2) - 2D_0(\text{CN}) - 10.7 \text{ e. v.} \quad (1)$$

The dissociation energy of cyanogen has been reported by Kistiakowsky and Gershinowitz¹⁶ to be 77 ± 4 kcal./mole, and by White¹⁷ to be 146 ± 4 kcal./mole. A chemical argument can be given that leads to an intermediate value. The dissociation energy of cyanogen may be expected to be greater than the carbon-carbon single-bond energy in diamond (one-half the heat of sublimation of diamond) by an amount equal to the conjugation energy of the two triple bonds in the molecule. This conjugation energy is twice that of two conjugated double bonds, with theoretical value¹⁸ 8 kcal./mole. The value of $D_0(\text{NC-CN})$ may hence be taken as 16 kcal./mole (0.70 e. v.) greater than one-half the heat of sublimation of diamond, and if this heat of sublimation lies between 125 and 170 kcal./mole the value of $D_0(\text{NC-CN})$ is calculated to be 90 ± 11 kcal./mole. Instead of using this value, with its large uncertainty, we may adopt the following procedure. Thermochemical data require that the value of $D_0(\text{CO})$ be 3.70 e. v. greater than the heat of sublimation of diamond, and hence, with the resonance energy 0.70 e. v. in cyanogen, we obtain the equation

$$D_0(\text{NC-CN}) = \frac{1}{2}D_0(\text{CO}) - 1.15 \text{ e. v.} \quad (2)$$

From (1) and (2) we obtain the equation

$$\frac{3}{2}D_0(\text{CO}) = 2D_0(\text{CN}) - D_0(\text{N}_2) + 9.55 \text{ e. v.} \quad (3)$$

This equation with the values given above for $D_0(\text{CN})$ and $D_0(\text{N}_2)$ leads to 9.77 e. v. for $D_0(\text{CO})$, and hence to 140 kcal/mole for the heat of sublimation of graphite and 86 kcal./mole for the dissociation energy of cyanogen.

The methods that we have used in reaching these values involve some novel ideas—the concept of valence-state energy and the postulate that the valence-state energy is usually nearly the same for an atom in different molecules, the use of linear extrapolation of vibrational levels to obtain the dissociation energies of molecules into atoms in their valence states, the use of conjugation energy for expressing a difference in dissociation energies—and their reliability and accuracy have not been extensively tested. From internal evidence it seems likely, however, that these methods when cautiously applied yield energy values that involve no larger errors than a few tenths of an electron-volt, and that they may be used with considerable confidence, as in the present paper, to select the correct ones from among alternative widely differing possible values of dissociation energies of molecules.

* Contribution No. 1297.

¹ Herzberg, G., *Chem. Rev.*, **20**, 145–167 (1937); *J. Chem. Phys.*, **10**, 306–307 (1942).

² Hagstrum, H. D., and Tate, J. T., *Phys. Rev.*, **59**, 354–370 (1941); Hagstrum, H. D., *Ibid.*, **72**, 947–963 (1947).

³ Coster, D., and Brons, F., *Physica*, **1**, 155–160 (1934).

⁴ Gaydon, A. G., and Penney, W. G., *Proc. Roy. Soc. London*, **183A**, 374–388 (1944).

⁵ Brewer, L., Gilles, P. W., and Jenkins, F. A., *J. Chem. Phys.*, **16**, 797–807 (1948).

⁶ Long, L. H., *Ibid.*, **16**, 1087 (1948).

⁷ Voge, H. H., *Ibid.*, **16**, 984–986 (1948).

⁸ Brewer, L., *Ibid.*, **16**, 1165–1166 (1948).

⁹ Pauling, L., *Z. Naturforschung*, **3A**, 438–447 (1948).

¹⁰ Pauling, L., *Proc. Natl. Acad. Sci.*, **35**, 229–232 (1949).

¹¹ Mulliken, R. S., *Phys. Rev.*, **46**, 144–146 (1934).

¹² Wulf, O. R., *Ibid.*, **46**, 316 (1934).

¹³ Hagstrum, H. D., *J. Chem. Phys.*, **16**, 848–849 (1948).

¹⁴ Gaydon, A. G., *Dissociation Energies*, Chapman and Hall, Ltd., London, 1947.

¹⁵ *Ibid.*, p. 182.

¹⁶ Kistiakowsky, G. B., and Gershinowitz, H., *J. Chem. Phys.*, **1**, 432–439, 885 (1933).

¹⁷ White, J. U., *Ibid.*, **8**, 459–465 (1940).

¹⁸ Pauling, L., and Sherman, J., *Ibid.*, **1**, 679–686 (1933).

B. The Energies of the Valence States of Several Atoms
and the Valence State Dissociation Limits of Several
Diatomic Molecules

It has long been known that there is an almost universal tendency for the rate of convergence of vibrational energy levels of diatomic molecules to be an almost linear function of the vibrational quantum number, at least for the low-lying vibrational states. This simple, linear relationship is used frequently to predict, by linear extrapolation, dissociation energies of diatomic molecules, with the recognition of the fact that such a linear extrapolation to convergence of the vibrational levels according to the method of Birge and Sponer⁽¹⁾ usually predicts too large a dissociation energy. A critical discussion of the Birge-Sponer Extrapolation has been given recently by Gaydon⁽²⁾.

The significance of the difference in the dissociation energy found by linear extrapolation and the true dissociation energy has been pointed out recently by Pauling^(3,4). According to his interpretation, the dissociation energy found by linear extrapolation is to be identified with the energy of dissociation to atoms in their valence states, the valence state of an atom being defined as that atomic state in which the atom has the same electronic structure as it has in the molecule. The energy of the valence state of bivalent oxygen as it exists in O_2 , OH, and H_2O has been evaluated by Pauling⁽⁴⁾ as 0.74 ± 0.05 e.v., a value which is essentially the same as that predicted by Mulliken⁽⁵⁾, 0.67 e.v..

This energy of the valence state is found to be almost independent of the particular molecule in which bivalent oxygen is located⁽⁴⁾. The assumption that the energy of the valence state of most other atoms is similarly independent of the particular molecule but dependent on the valence state often allows the prediction of true dissociation energies which are more accurate than those which could be found by linear or non-linear extrapolation by the method of Birge and Sponer. And when several accurate, but widely differing, values of a true dissociation energy are possible, the value predicted by use of the concept of the valence state energy should resolve the ambiguity.

In Table I are given the values of the dissociation energies of several diatomic molecules as found by linear graphical extrapolation. Values of the increments of vibrational energy were determined from band heads or band origins of electronic transitions reported in the literature. Since a thorough search of the literature was made for all the molecules of Table I, a complete list of references would be long. An entry to the literature, however, may be gained readily by reference to Gaydon⁽²⁾ or Herzberg⁽⁶⁾. Almost all increments of vibrational energy so found for each electronic state were plotted against the average vibrational quantum number, and the straight line judged by eye to be the best was drawn through these points. From the intercepts on the axes, the linearly extrapolated dissociation energy from the lowest vibrational state of each electronic state was calculated, this energy being given by the area beneath the straight

TABLE I

Valence State Dissociation Limits

AB	State	D_0' (extrap)	A_0	$D_0' + A_0$	States of Products		Energy of Products (e.v.)	Limit (e.v.)
		(e.v.)	(e.v.)	(e.v.)	A	B		
OH	$X^2\Pi$	5.01	0.00	5.01	3P	2S	0.00	5.01
	$A^2\Sigma^+$	3.02	4.02	7.04	1D	2S	1.97	5.07
O ₂	$X^3\Sigma^-$	6.69	0.00	6.69	3P	3P	0.00	6.69
	$a^1\Delta_g$	5.38	0.98	6.36	3P	3P	0.00	6.36
	$b^1\Sigma_g^-$	4.42	1.63	6.05	3P	3P	0.00	6.05
	$A^3\Sigma^-$	1.09	4.43	5.52	3P	3P	0.00	5.52
	$B^3\Sigma^-$	1.81*	6.12	7.93	3P	1D	1.97	5.96
SO	$X^3\Sigma^-$	6.31*	0.00	6.31	3P	3P	0.00	6.31
	$B^3\Sigma^-$	2.13*	4.85	6.98	1D	3P	1.14	5.84
S ₂	$X^3\Sigma^-$	5.60	0.00	5.60	3P	3P	0.00	5.60
	$B^3\Sigma^-$	2.04	3.93	5.97	1D	3P	1.14	4.83
NO	$X^2\Pi$	7.87	0.00	7.87	4S	3P	0.00	7.87
	$A^2\Sigma^+$	11.71	5.47	17.18	4S	5S	9.14	8.04
	$B^2\Pi$	4.72	5.62	10.34	2D	3P	2.38	7.96
	$D^2\Sigma^+$	6.87	6.60	13.47	2P	1D	5.54	7.93
NS	$X^2\Pi$	6.29	0.00	6.29	4S	3P	0.00	6.29
N ₂	$X^1\Sigma^+$	11.60	0.00	11.60	4S	4S	0.00	11.60
	$A^3\Sigma_g^+$	4.36	6.17	10.53	4S	4S	0.00	10.53
	$B^3\Pi_g$	6.23	7.35	13.58	2D	4S	2.38	11.20
	$a^1\Pi_g$	6.23	8.54	14.77	2D	2D	4.76	10.01
	$C^3\Pi_g$	2.11**	11.03	13.14	2D	4S	2.38	10.76
CO	$X^1\Sigma^+$	11.23	0.00	11.23	3P	3P	0.00	11.23
	$a^3\Pi$	6.38	6.01	12.39	1D	3P	1.26	11.13
	$d^3\Pi$	4.34	7.66	12.00	1D	3P	1.26	10.74
	$A^1\Pi$	4.07	8.02	12.09	3P	3P	0.00	12.00
	$B^1\Sigma^+$	3.84	10.78	14.62	1D	1D	3.23	11.39
CS	$X^1\Sigma^+$	8.01	0.00	8.01	3P	3P	0.00	8.01
	$A^1\Pi$	3.25	4.81	8.06	3P	3P	0.00	8.06
CN	$X^2\Sigma^+$	8.94	0.00	8.94	3P	4S	0.00	8.94
	$A^2\Pi$	7.81	1.13	9.94	3P	4S	0.00	9.94
	$B^2\Sigma^+$	7.27	3.20	10.47	3P	2D	2.38	8.09
CP	$X^2\Sigma^+$	6.95	0.00	6.95	3P	4S	0.00	6.95
	$A^2\Pi$	5.60	2.73	8.33				
	$B^2\Sigma^+$	3.56	3.58	7.14				
CO ⁺	$X^2\Sigma^+$	10.12	0.00	10.12				
	$A^2\Pi$	6.30	2.53	8.83				
	$B^2\Sigma^+$	3.61	5.66	9.27				
N ₂ ⁺	$X^2\Sigma^+$	8.94	0.00	8.94				
	$B^2\Sigma_g^+$	6.20*	3.17	9.37				
O ₂ ⁺	$X^2\Pi_g$	6.58	0.00	6.58				
	$A^2\Pi_g$	1.83	4.74	6.57				

* Mathematical linear extrapolation(6).

** Graphical non-linear extrapolation.

line. The values found in this way are reported in Table I. The fourth column of this table contains the energies of the various electronic states above the ground electronic states, and the fifth column contains the height of the various valence state dissociation limits above the ground state. Values of these limits have been calculated previously by Pauling⁽³⁾. Several of these dissociation limits coincide for most of the molecules, and if reasonable amounts of atomic excitation energy, as indicated in columns six and seven of Table I, are subtracted from these limits, then these valence state dissociation limits are generally brought into coincidence. The limit which corresponds to dissociation to atoms in their valence states is taken to be the average of these almost coinciding limits, values of this limit for the various molecules being given in Table II. For CP, CO⁺, N₂⁺, and O₂⁺, an obvious correlation with excited and unexcited atoms as allowed by the correlation rules does not exist.

In Table II a calculation of the valence state energies of O, S, N, and C is illustrated for several assumptions about true dissociation energies, these assumptions differing only slightly from those made previously^(3,4,7). The values of columns three to six of Table II are derived line by line from top to bottom by assuming the values enclosed in parentheses. Other sets of values of the dissociation energies for N₂, NO, CO, and CN and for SO and S₂ might have been assumed, but such assumptions lead to valence state energies which differ rather markedly from values expected theoretically⁽⁵⁾. For example, the valence state energy of S is predicted to be

TABLE II

Valence State Energies of Atoms

Molecule AB	Limit (e.v.)	D ₀ (e.v.)	Total V.S.E. (e.v.)	V.S.E. of A (e.v.)	of B (e.v.)
OH	5.04	(4.40)	0.64	0.64	0.00
O ₂	6.12	(5.08)	1.04	0.52	0.52
SO	6.07	(5.15)	0.92	0.40	(0.52)
S ₂	5.22	(4.4)	0.8	0.4	0.4
N ₂	10.83	(7.37)	3.46	1.73	1.73
NO	7.95	(5.29)	2.66	2.1	(0.6)
NS	6.29	4.1	2.2	(1.8)	(0.4)
CO	11.30	(9.6)	1.7	1.1	(0.6)
CS	8.04	6.5	1.5	(1.1)	(0.4)
CN	8.99	6.1	2.9	(1.1)	(1.8)

somewhat less than the value for oxygen; hence, a value of $D_0(S_2)$ of less than 4.0 e.v. is unacceptable. Table II illustrates the usefulness of the valence state energy: values of $D_0(NS)$ and $D_0(CS)$ are predicted, and the value predicted for $D_0(CN)$, namely 6.1 e.v., is in good agreement with the lower of the two spectroscopically favored values, 6.25 e.v. and 7.50 e.v.^(2,6).

References of Section III

1. R. T. Birge and H. Sponer, Phys. Rev., 28, 259 (1926).
2. A. G. Gaydon, Dissociation Energies, Chapman and Hall Ltd., London (1947).
3. L. Pauling, Z. Naturforsch., 3A, 438 (1948).
4. L. Pauling, Proc. Nat. Acad. Sci. U.S., 35, 229 (1949).
5. R. S. Mulliken, J. Chem. Phys., 2, 789 (1934).
6. G. Herzberg, Molecular Spectra and Molecular Structure I. Spectra of Diatomic Molecules, second ed., D. van Nostrand Co., Inc., N. Y. (1950).
7. Section III A of this thesis: L. Pauling and W. F. Sheehan, Jr., Proc. Nat. Acad. Sci. U.S., 35, 359 (1949).

PROPOSITIONS

1. The variation in the increments in the molar refraction per CH_2 -group in SiR_4 , GeR_4 , and $\text{Si}(\text{SR})_4$ ⁽¹⁾ may be explained on the basis of hyperconjugation and consequent optical exaltation.

2. Anharmonicity in the symmetrical stretching modes of vibration in polyatomic molecules allows the calculation, by a linear Birge-Sponer-like extrapolation⁽²⁾, of a dissociation energy to atoms in their valence states⁽³⁾.

3. Some miscellaneous uses of the valence-state dissociation limits^(4,5) are:

- a) to calculate one of the three quantities w_e , $x_e w_e$, and A_0 .
- b) to detect avoided crossing of potential curves and great resonance interaction. An example of an avoided crossing is the pair of Σ^+ states of CO^+ ; examples of resonance are N_2^+ and O_2^+ .

4. Equation 12c of reference (6) expresses the radii of the platinum transition metals as a function of bond order, d-character, and atomic number. A modification of this equation, giving the radii of all the elements of the very long period in a similar functional relationship, is

$$R_1(\delta, \delta', \emptyset, z) = 2.019 - 0.019z - (1.321 - 0.037z)\delta - (0.175 - 0.005z)\delta' - (0.297 - 0.008z)\emptyset$$

where

$$\begin{aligned} \delta &= 5d\text{-character} \\ \delta' &= 6d\text{-character} \\ \emptyset &= 4f\text{-character (1.00 or 0.00)} \\ z &= Z - 54. \end{aligned}$$

5. Knowledge of the structures of OsF_8 and HfF_4 would be of interest towards the understanding of the unusual structures of OsO_4 ⁽⁵⁾, $\text{Mo}(\text{CO})_6$ ⁽⁵⁾, $\text{W}(\text{CO})_6$ ⁽⁵⁾, MoF_6 ⁽⁷⁾, WF_6 ⁽⁷⁾, and UF_6 ^(7,8).

6. Braune and Stute⁽⁹⁾ have reported the existence of two different metal-oxygen distances in both OsO_4 (1.79Å and 2.81Å) and RuO_4 (1.66Å and 2.74Å). It seems probable, in view of the recent determination of the structure of OsO_4 ⁽⁵⁾, that these investigators have observed mean metal-oxygen distances and oxygen-oxygen distances. Accordingly, the structure of RuO_4 is probably analogous to OsO_4 , with RuO equal to 1.60Å and 1.73Å.

7. a) A study of the kinetics of the reaction $\text{N}^{14}\text{N}^{14} + \text{N}^{15}\text{N}^{15} \rightarrow 2\text{N}^{14}\text{N}^{15}$ may indicate the magnitude of $D_0(\text{N}_2)$.

b) The detection of $\text{N}^{14}\text{N}^{15}$ resulting from the quenching of fluorescence of $\text{Kr} (4s^2 4p^5 5s)$ or $\text{Xe} (5s^2 5p^5 6s)$ by a mixture of $\text{N}^{14}\text{N}^{14}$ and $\text{N}^{15}\text{N}^{15}$ may fix the value of $D_0(\text{N}_2)$.

8. The existence of nuclear excitation energies of the order of 2 volts, though improbable, may be experimentally observed by the observation of forbidden rotational states in X_2 diatomic molecules (for example, N_2) at elevated temperatures.

REFERENCES FOR PROPOSITIONS

1. K. Fajans, Chem. & Eng. News, 27, 900 (1949).
2. R. T. Birge and H. Sponer, Phys. Rev., 28, 259 (1926).
3. See, for example, L. Pauling, Proc. Nat. Acad. Sci. U.S., 35, 229 (1949).
4. L. Pauling, Z. Naturforsch., 3A, 438 (1948).
5. W. F. Sheehan, Jr., Thesis, California Institute of Technology, 1952.
6. L. Pauling, Proc. Roy. Soc., A196, 343 (1949).
7. O. Bastiansen, unpublished.
8. S. H. Bauer, J. Chem. Phys., 18, 27 (1950).
9. H. Braune and K. W. Stute, Angew. Chem., 51, 528 (1938).